

Avoiding barren plateaus via Gaussian Mixture Model

Xiao Shi^{1,2} and Yun Shang^{1,3,*}

¹*Institute of Mathematics, Academy of Mathematics and Systems Science, Chinese Academy of Sciences, Beijing 100190, China*

²*School of Mathematical Sciences, University of Chinese Academy of Sciences, Beijing 100049, China*

³*NCMIS, MDIS, Academy of Mathematics and Systems Science, Chinese Academy of Sciences, Beijing, 100190, China*

(Dated: February 22, 2024)

Variational quantum algorithms is one of the most representative algorithms in quantum computing, which has a wide range of applications in quantum machine learning, quantum simulation and other related fields. However, they face challenges associated with the barren plateau phenomenon, especially when dealing with large numbers of qubits, deep circuit layers, or global cost functions, making them often untrainable. In this paper, we propose a novel parameter initialization strategy based on Gaussian Mixture Models. We rigorously prove that, the proposed initialization method consistently avoids the barren plateaus problem for hardware-efficient ansatz with arbitrary length and qubits and any given cost function. Specifically, we find that the gradient norm lower bound provided by the proposed method is independent of the number of qubits N and increases with the circuit depth L . Our results strictly highlight the significance of Gaussian Mixture model initialization strategies in determining the trainability of quantum circuits, which provides valuable guidance for future theoretical investigations and practical applications.

Introduction.—In recent years, the rapid advancement of quantum computing technology has drawn attention to Variational Quantum Algorithms (VQAs)[1–3] as a promising quantum algorithm with broad application prospects. In the current era of Noisy Intermediate-Scale Quantum (NISQ) devices[4–6], VQAs provides a feasible approach to solving complex problems, where challenges such as noise and errors in quantum computing devices make large-scale fully quantum computations difficult[7–10]. On the other hand, VQAs utilizes Parametrized Quantum Circuits (PQCs), denoted as $V(\theta)$, as its quantum computing framework. PQCs serving as a trainable model adjusts its parameters θ through classical optimization to minimize or maximize a specified cost function. By employing parametrized quantum circuits, VQAs can adapt flexibly to the characteristics of different problems, providing a robust and practical option for quantum computation on NISQ devices[11–14]. VQAs exhibit immense potential across a spectrum of applications, showcasing efficient quantum algorithms that excel in tasks ranging from chemical molecular structure and energy calculations [15–17] to combinatorial optimization problems[18, 19] and machine learning[20–23]. These applications not only have profound implications for scientific research but also offer innovative solutions for practical applications.

Training VQAs encompasses various methodologies, including gradient-based[24, 25] and gradient-free[26, 27] approaches. However, regardless of the sampling method employed, it is susceptible to encountering the notorious barren plateaus (BP) problem[28–30]. The phenomenon of the barren plateau is characterized by the randomized initialization of parameters θ in VQAs, leading to an exponential vanishing of the cost function gradient along any direction with the increasing number of qubits. The genesis of this challenge lies in the intricacies of entanglement within quantum circuits[31]. Numerous strategies have emerged to address this issue, such as optimizing initialization policies[32–35], refining circuit structures[36–38], or employing local cost functions[29, 30].

The design of the circuit ansatz is crucial for capturing quantum correlations, including physics-inspired[11, 39, 40] and hardware-efficient ansatz designs[41]. While physics-inspired ansatz exhibits some advantages in certain aspects[40, 42], they also face serious challenges in terms of computational resources. On the other hand, hardware-efficient ansatz[16] caters to the limitations of NISQ devices, striking a balance between achievability and performance. The quest for an effective solution to mitigate BP and enhance the versatility of addressing linear combinations in the context of a hardware-efficient ansatz continues to be a forefront challenge in the training of VQAs.

The Gaussian Mixture Model (GMM)[43] is a probability distribution model composed of multiple Gaussian distributions. Each Gaussian distribution, referred to as a component, contributes to the overall mixture distribution. Every component is characterized by its own mean, variance, and weight. This versatile model finds widespread applications in statistics and machine learning[44–46], particularly in tasks such as clustering[47, 48], density estimation[49], and generative modeling[50]. GMM excels at fitting complex data distributions and, owing to its flexibility and expressive power, is frequently employed for modeling diverse categories of data.

In the training of VQAs, the parameter update expression for the cost function $f(\theta)$ based on gradient optimization methods is $f(\theta_{k+1}) = f(\theta_k) - \alpha \|\nabla_{\theta} f(\theta_k)\|_2^2 + o(\alpha)$, where $\theta_{k+1} = \theta_k - \alpha \nabla_{\theta} f(\theta_k)$, α is the learning rate. Therefore, typically $\|\nabla_{\theta} f(\theta)\|_2^2$ is used to determine whether the cost function $f(\theta)$ can be updated. In this letter, we employ GMM for parameter initialization in VQAs to address the barren plateau problem. Considering arbitrary observables O which can be a single term or a linear combination of terms, by designing specific GMM initialization methods based on O , we rigorously prove the following conclusions: (1) When the observable O consists of a single term, the lower bound of $\|\nabla_{\theta} f(\theta)\|_2^2$ is independent of the number of quantum bits N and increases with the circuit length; (2) When O is a linear

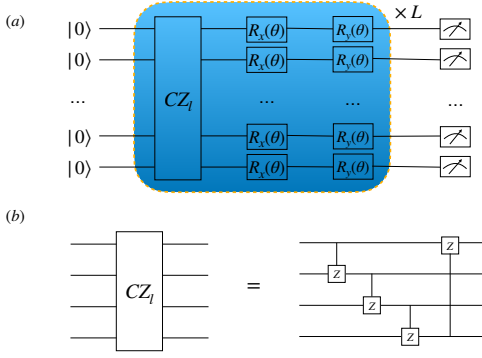


FIG. 1. (a) The fundamental framework of the variational quantum circuit, comprising L blocks. Each block begins with the introduction of entanglement through CZ_l gates, followed by the application of R_x and R_y gates on each qubit. The structure of CZ_l is depicted in (b).

combination of many terms, the lower bound of $\|\nabla_{\theta} f(\theta)\|_2^2$ increases compared to the single-term case and not decrease; (3) When \mathbf{O} consists of non-negative terms, by adjusting GMM, we may achieve a larger lower bound. Therefore, the barren plateau problem does not occur in these scenario, and the model can undergo effective training. This is significant for reducing the cost and saving quantum resources during model training. Additionally, numerical experiments show excellent performance for both local and global cost functions using our method.

Notations and framework.—The probability density function of the GMM can be expressed as a weighted sum of individual components. Assuming there are K components, for a given one-dimensional variable x , the GMM's probability density function can be represented as:

$$p(x) = \sum_{i=1}^K \pi_i \cdot \mathcal{N}(x|\mu_i, \sigma_i^2) \quad (1)$$

where K is the number of Gaussian components, π_i is the weight of the i th component, satisfying $\sum_{i=1}^K \pi_i = 1$, $\mathcal{N}(x|\mu_i, \sigma_i^2)$ is the probability density function of the i th Gaussian component, with mean μ_i and variance σ_i^2 . Here are a few rules. Let \mathcal{G}_0 be an arbitrary distribution, and if the random variable θ follows any distribution, it can be expressed as $\theta \sim \mathcal{G}_0$. Furthermore, $\mathcal{G}_1(\sigma^2)$ denotes the Gaussian distribution $\mathcal{N}(0, \sigma^2)$. $\mathcal{G}_2(\sigma^2)$ denotes the first GMM we used, where its probability density function is $p(x) = \frac{1}{2}\mathcal{N}(x|-\frac{\pi}{2}, \sigma^2) + \frac{1}{2}\mathcal{N}(x|\frac{\pi}{2}, \sigma^2)$. Similarly, $\mathcal{G}_3(\sigma^2)$ is the second GMM, where its probability density function is $p(x) = \frac{1}{4}\mathcal{N}(x|-\pi, \sigma^2) + \frac{1}{4}\mathcal{N}(x|\pi, \sigma^2) + \frac{1}{2}\mathcal{N}(x|0, \sigma^2)$.

In this letter, we employ the ansatz illustrated in Fig. 1, which is a typical hardware-efficient ansatz. It involves N qubits and L blocks. Its objective is to minimize the cost function $f(\theta) = \text{Tr}[\mathbf{O}V(\theta)\rho_{in}V^\dagger(\theta)]$ by optimizing the parameters θ within the circuit. Here, \mathbf{O} is an observable, $V(\theta)$ is

a parameterized quantum circuit, and ρ_{in} is the input quantum state. We assume ρ_{in} is a pure state. In most cases, $\rho_{in} = |\mathbf{0}\rangle\langle\mathbf{0}|$ and $|\mathbf{0}\rangle = |0\rangle^{\otimes N}$. For an arbitrary observable $\mathbf{O} = o_1 \otimes o_2 \otimes \dots \otimes o_N$, where $o_i \in \{I, X, Y, Z\}$. We define $I_S := \{n|o_n \neq I, n \in [N]\}$, representing the set of qubits where the observable acts nontrivially, and there are S elements in this set[32, 33].

When there are two observables $\mathbf{O}_i = o_1^i \otimes o_2^i \otimes \dots \otimes o_N^i$ and $\mathbf{O}_j = o_1^j \otimes o_2^j \otimes \dots \otimes o_N^j$, for all $m \in [N]$, the Pauli matrices at the m -th position are denoted by o_m^i and o_m^j . We provide the following definitions:

$$S_3^{ij} := |\{m|o_m^i = o_m^j = Z, m \in [N]\}| \quad (2)$$

$$S_{1:3}^{ij} := |\{m|o_m^i = o_m^j \neq I, m \in [N]\}| \quad (3)$$

$$S_{0,3}^{ij} := |\{m|o_m^i = I, o_m^j = Z || o_m^i = Z, o_m^j = I, m \in [N]\}|. \quad (4)$$

Main results.—We begin by considering the case where the observable consists of only one term, which can be either global or local. Previous research has indicated that avoiding the barren plateau problem for global observables is challenging[30, 51, 52]. Nevertheless, regardless of the specifics, we will rigorously prove that it does not encounter the barren plateau problem when we adopt the GMM as the parameter initialization strategy. The ansatz that we consider is shown in Fig. 1. Here, parameters in different blocks will be initialized using distinct methods, and the initialization approach is determined based on the observable \mathbf{O} . For convenience, as illustrated in Table I, we adopt a tabular format to describe the distribution of the parameter θ in the final block. Now, let's formulate our first theorem.

TABLE I. On the i -th qubit, the parameters in $R_y(\theta)$ and $R_x(\theta)$ are intricately designed, dynamically adjusted based on the distinct Pauli matrices of the observable. When o_i corresponds to Z , there are two possible choices for the parameters in R_x and R_y .

o_i	X	Y	Z	I
Init method of R_y	$\mathcal{G}_2(\sigma^2)$	\mathcal{G}_0	$\mathcal{G}_1(\sigma^2)/\mathcal{G}_3(\sigma^2)$	\mathcal{G}_0
Init method of R_x	$\mathcal{G}_1(\sigma^2)$	$\mathcal{G}_2(\sigma^2)$	$\mathcal{G}_1(\sigma^2)/\mathcal{G}_3(\sigma^2)$	\mathcal{G}_0

Theorem 1. Consider a VQAs problem defined above, assuming that the parameters θ in the last block defined in Table I, and the parameters θ of the remaining blocks obey the distribution $\mathcal{G}_1(\sigma^2)$, where $\sigma^2 = \frac{1}{2LS}$. Then $\forall q \in \{1, \dots, 2L\}, n \in \{1, \dots, N\}$, we have

$$\mathbb{E}_{\theta} \partial_{\theta_{q,n}} f(\theta) = 0 \quad (5)$$

$$\mathbb{E}_{\theta} \|\nabla_{\theta} f(\theta)\|_2^2 \geq \frac{1}{4} - \frac{1}{8L} \quad (6)$$

where $\nabla_{\theta} f(\theta)$ denotes the gradient of function $f(\theta)$ about θ .

Proof. The main idea is outlined here, with the detailed proof provided in the Supplementary Materials[53]. We expand the quantum state ρ_{out} by the PQC layer by layer. In the last block, due to our specially designed distribution, a coefficient of zero will always be generated, resulting in an expectation of zero, yielding Eq. (5). We find that $\mathbb{E}_{\theta} \|\nabla_{\theta} f(\theta)\|_2^2$ can be

expanded into a sum of terms composed of $\text{Tr}^2[\mathbf{O}_i \rho_0]$, with coefficients determined by the powers of $\alpha = \mathbb{E}_{\theta \sim \mathcal{G}_1(\sigma^2)} \cos^2 \theta$

and $\beta = \mathbb{E}_{\theta \sim \mathcal{G}_1(\sigma^2)} \sin^2 \theta$. Among these terms, we select the one with only I or Z that has the largest coefficient. Considering that in this case $\text{Tr}^2[\mathbf{O}_i \rho_0] = 1$, the lower bound of the gradient norm is then determined by the lower bound of this coefficient, leading to the derivation of Eq. (6) and complete the proof. \square

The above theorem indicates that, employing our initialization method, the issue of barren plateaus can be consistently avoided, regardless of whether the cost function is global or local. From Eq. (6), it is evident that our norm has a constant lower bound of $\frac{1}{8}$. This is in stark contrast to the exponential lower bound ($O(\frac{1}{L^N})$) found in previous works for global cost functions [32, 33]. The utilization of GMM significantly improves this lower bound. Additionally, we observe that for certain specific observables, not all parameters θ in the circuit impact the final value of the cost function $f(\theta)$. We refer to those θ parameters that do not affect the cost function as "inactive parameters", while the others are named "active parameters". More details can be found in the supplementary materials[53]. Using a similar approach, we can also demonstrate that when the cost function is global, for all active parameters $\theta_{q,n}$, $\text{Var} \partial_{\theta_{q,n}} f(\theta) \geq \frac{1}{8LN}$. This provides an additional perspective on how our method enables escape from the barren plateau.

When our observable is composed of a linear combination of many terms rather than a single term, the cost function can be expressed as $f(\theta) = \text{Tr} \left[\left(\sum_i \mathbf{O}_i - \sum_j \mathbf{O}_j \right) U(\theta) \rho_{\text{in}} U(\theta)^\dagger \right]$, where \mathbf{O}_i and \mathbf{O}_j are single terms. Here we randomly select one term from the observable to construct the initialization method. The construction of the last block is detailed in Table II. Suppose there are S nontrivial Pauli matrices in the selected \mathbf{O}_k . Additionally, there are M terms that differ from \mathbf{O}_k only by replacing Pauli Z with the identity matrix I or vice versa among \mathbf{O}_i and \mathbf{O}_j at corresponding positions (including the original \mathbf{O}_k itself). As before, the PQC is illustrated in Fig. 1. Now we present our Theorem 2.

TABLE II. On the i -th qubit, the parameters in $R_y(\theta)$ and $R_x(\theta)$ are intricately designed, dynamically adjusted based on the distinct Pauli matrices of the observable.

o_i	X	Y	Z	I
Init method of R_y	$\mathcal{G}_2(\sigma^2)$	$\mathcal{G}_1(\sigma^2)$	$\mathcal{G}_3(\sigma^2)$	$\mathcal{G}_3(\sigma^2)$
Init method of R_x	$\mathcal{G}_1(\sigma^2)$	$\mathcal{G}_2(\sigma^2)$	$\mathcal{G}_3(\sigma^2)$	$\mathcal{G}_3(\sigma^2)$

Theorem 2. Considering the above definition of the cost function, let the parameters of the L -th block in the ansatz be defined as shown in Table II. The parameters in the preceding $L-1$ blocks all follow a Gaussian distribution $\mathcal{G}_1(\sigma^2)$, where $\sigma^2 = \frac{1}{2LS}$. With these considerations, we obtain a lower bound on its squared norm of the gradient:

$$\mathbb{E}_{\theta} \|\nabla_{\theta} f(\theta)\|_2^2 \geq M \left(\frac{1}{4} - \frac{1}{8L} \right) \quad (7)$$

Proof. We give the main idea here. The detailed proof is technically involved and thus left to the Supplementary Materials[53]. Since the distributions for Z and I are the same here, for \mathbf{O}_k itself or by just changing Z to I or I to Z in \mathbf{O}_k , it can undergo a similar proof using Theorem 1. As for other quadratic terms, they are evidently greater than or equal to 0. For any cross terms, when expanded into a series of summations, it becomes apparent that each term is 0. Therefore, all cross terms are equal to 0. Thus, we obtain Eq. (7) and complete the proof. \square

From Theorem 2, it can be observed that as the number of terms increases, even if there are some terms with negative coefficients, the lower bound on its norm might become larger. This enables us to update the parameters more effectively. However, when we face a situation where the coefficients in its loss are all non-negative, we propose a new initialization method that can provide a larger lower bound in certain specific cases. Assuming our cost function at this stage is $f(\theta) = \text{Tr} \left[\sum_i \mathbf{O}_i U(\theta) \rho_{\text{in}} U(\theta)^\dagger \right]$. Once again, we randomly select a term $\mathbf{O}_{k'}$, and following the previous notation, let S denote the number of non-identity matrices in $\mathbf{O}_{k'}$. We determine the distribution of θ in the final layer based on the Pauli matrices in $\mathbf{O}_{k'}$, as shown in Table III. As before, we assume that among the remaining terms, there are M terms that differ from $\mathbf{O}_{k'}$ only by replacing Pauli Z with the identity matrix I or vice versa at corresponding positions (including the original $\mathbf{O}_{k'}$ itself). We denote the set of indices satisfying these conditions, along with k' , as \mathcal{K} . Next, we present our Theorem 3.

TABLE III. On the i -th qubit, the parameters in $R_y(\theta)$ and $R_x(\theta)$ are intricately designed, dynamically adjusted based on the distinct Pauli matrices of the observable.

o_i	X	Y	Z	I
Init method of R_y	$\mathcal{G}_2(\sigma^2)$	$\mathcal{G}_1(\sigma^2)$	$\mathcal{G}_1(\sigma^2)$	$\mathcal{G}_1(\sigma^2)$
Init method of R_x	$\mathcal{G}_1(\sigma^2)$	$\mathcal{G}_2(\sigma^2)$	$\mathcal{G}_1(\sigma^2)$	$\mathcal{G}_1(\sigma^2)$

Theorem 3. In accordance with the aforementioned definition of the cost function, the parameters of the L -th block in the ansatz are defined as presented in Table III. The parameters in the preceding $L-1$ blocks all adhere to a Gaussian distribution $\mathcal{G}_1(\sigma^2)$, where $\sigma^2 = \frac{1}{2LS}$. With these considerations, we derive a lower bound on its norm:

$$\mathbb{E} \|\nabla_{\theta} f(\theta)\|_2^2 \geq M \left(\frac{1}{4} - \frac{1}{8L} \right) + \sum_{\substack{i,j \in \mathcal{K} \\ i \neq j}} \frac{(2L-1)S_3^{i,j}}{2LS} \left(1 - \frac{1}{2LS} \right)^{2LS^{i,j}} e^{-\frac{S_{0,3}^{i,j}}{2S}} \quad (8)$$

Since the proof is similar to Theorem 2, please refer to Supplementary Materials[53]. Theorem 3 informs us that when the objective function does not contain negative terms, compared to Theorem 2, we can achieve initialization for all parameters using only the distributions $\mathcal{G}_1(\sigma^2)$ and $\mathcal{G}_2(\sigma^2)$, no need for $\mathcal{G}_3(\sigma^2)$. Moreover, in specific cases, the lower bound on its norm is large or equal to the bound proposed in Theorem 2.

Experiments.—VQAs play a crucial role in various domains, including the modeling of quantum spins[54], quantum machine learning[55–57], and quantum chemistry[58–60]. In this section, we embark on a comprehensive exploration of our proposed method, drawing comparisons with existing approaches across the spectrum of local and global cost functions. This comparative analysis aims to illuminate the efficacy and adaptability of our strategy in diverse scenarios, shedding light on its potential to enhance quantum computational tasks in both theoretical modeling and practical applications.

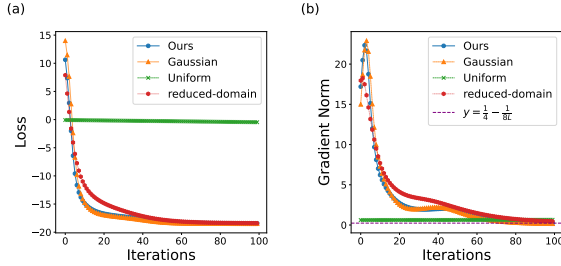


FIG. 2. In the training process of the 1D Transverse Field Ising Model, the cost function and gradient norm undergo transformations. Since it is a local cost function, the majority of initialization methods converge to its minimum value.

First, we initially focus on a local observable in the 1D transverse field Ising model (TFIM)[61, 62], described by the Hamiltonian $H_{\text{TFIM}} = \sum_{i,i+1} Z_i Z_{i+1} - \sum_i X_i$. Setting the initial state $\rho_{in} = |0\rangle\langle 0|$, with $N = 15$, and $L = 15$, we aim to compute the ground state of the system. We choose the observable $X_1 \otimes I_2 \otimes \dots \otimes I_N$ to initialize the circuit parameters. In addition, we compare our proposed method with existing initialization strategies, such as the uniform distribution $\mathcal{U}[-\pi, \pi]$, Gaussian distribution $\mathcal{N}(0, \frac{1}{4S(L+2)})$, and the reduced-domain distribution $\mathcal{U}[-a\pi, a\pi]$, where a is set to 0.07. The experimental results are illustrated in Figure 2, where (a) depicts the variation of the cost function during the training process, and (b) shows the ℓ_2 norm of corresponding gradients throughout the optimization. Considering that choosing the observable $Z_1 \otimes Z_2 \otimes \dots \otimes I_N$ for initial-

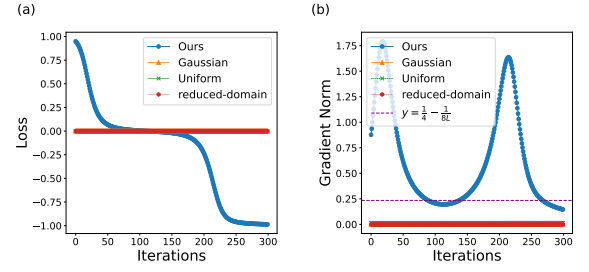


FIG. 3. In the training process, when the observable is entirely composed of X , the cost function and gradient norm undergo transformations. The gradients for Gaussian, uniform, and reduced-domain distributions remain near zero, resulting in almost non-decreasing cost functions for these distributions. In contrast, our method maintains relatively large gradients throughout the training process and is able to descend to the final results.

ization could also involve initializing all parameters with a Gaussian distribution, our proposed method offers a broader range of distribution choices. The reduced-domain distribution, similar to the Gaussian distribution, concentrates data around zero. Consequently, our method, along with Gaussian distribution and reduced-domain distribution, proves effective in finding the ground state, significantly outperforming the uniform distribution $\mathcal{U}[-\pi, \pi]$.

However, Gaussian and reduced-domain distributions do not always perform well. For instance, on global cost functions, they can only provide exponential lower bounds, which can not avoid the barren plateau problem in general. Now, we consider the cost function $f(\theta) = \text{Tr}[\mathbf{O}U(\theta)\rho_{in}U^\dagger(\theta)]$, where $\mathbf{O} = X_1 \otimes X_2 \otimes \dots \otimes X_N$, $\rho_{in} = |0\rangle\langle 0|$. We set $N = 20$ and $L = 8$, the results are depicted in Figure 3. Clearly, in this scenario, neither the Gaussian distribution nor the uniform distribution can induce parameter updates, as their gradient norms tend towards zero. In contrast, our method’s gradient norm starts with an initial value greater than $\frac{1}{4} - \frac{1}{8L} \approx 0.23$, significantly surpassing others. Moreover, the gradient norm remains within a relatively large range throughout the entire training process. This enables our approach to escape what is commonly referred to as the vanishing gradient problem on plateaus. The observations align perfectly with the conclusions derived from Theorem 1.

We further validated our approach on arbitrary global cost functions and in the context of quantum chemistry, considering the impact of noise on our results. Detailed experimental procedures are provided in the supplementary materials[53]. The source code for numerical results is available on [63].

Conclusion.—In this paper, we introduce GMM into the parameter initialization of PQCs to circumvent the notorious barren plateau problem. Results indicate the universality of our approach, as it applies to various cost functions, and we rigorously prove that its gradient norms is no less than $\frac{1}{8}$. We validate our algorithm for diverse problems, which is crucial for VQAs as it enables the training of larger and deeper quantum circuits, unlocking the potential of quantum computation. Especially, it is worth noting that our approach is not limited

to the specific structure of quantum circuits. Further details are available in the supplementary materials[53].

While the theorems presented in our paper are tailored to the ansatz in Fig. 1, the applicability of our theorems and proof techniques can extend to other ansatz structures. Furthermore, considering the analogous BP issues in tensor network simulations[30, 64], we anticipate incorporating our method into the initialization of tensor networks in the future. However, due to the sharp- P completeness of classical simulations in tensor networks, even without facing BP, computing their derivatives remains challenging for large-scale problems. In contrast, VQAs can efficiently obtain expected values through quantum devices, making them implementable. Certainly, for effective training of VQAs, overcoming the barren plateau is just one step, as they still face challenges such as local minima[65, 66] that need to consider.

We thank helpful discussion with Yabo Wang and Tianen Chen. This work was supported by the National Key R&D Program of China (Grant No. 2023YFA1009403), the National Natural Science Foundation special project of china (Grant No.12341103) and National Natural Science Foundation of China (Grant No. 62372444).

* shangyun@amss.ac.cn

- [1] J. R. McClean, J. Romero, R. Babbush, and A. Aspuru-Guzik, The theory of variational hybrid quantum-classical algorithms, *New Journal of Physics* **18**, 023023 (2016).
- [2] C. Cîrstoiu, Z. Holmes, J. Iosue, L. Cincio, P. J. Coles, and A. Sornborger, Variational fast forwarding for quantum simulation beyond the coherence time, *npj Quantum Information* **6**, 82 (2020).
- [3] M. Cerezo, K. Sharma, A. Arrasmith, and P. J. Coles, Variational quantum state eigensolver, *npj Quantum Information* **8**, 113 (2022).
- [4] K. Bharti, A. Cervera-Lierta, T. H. Kyaw, T. Haug, S. Alperin-Lea, A. Anand, M. Degroote, H. Heimonen, J. S. Kottmann, T. Menke, W.-K. Mok, S. Sim, L.-C. Kwek, and A. Aspuru-Guzik, Noisy intermediate-scale quantum algorithms, *Rev. Mod. Phys.* **94**, 015004 (2022).
- [5] A. Arrasmith, L. Cincio, A. T. Sornborger, W. H. Zurek, and P. J. Coles, Variational consistent histories as a hybrid algorithm for quantum foundations, *Nature Communications* **10**, 3438 (2019).
- [6] J. Preskill, Quantum Computing in the NISQ era and beyond, *Quantum* **2**, 79 (2018).
- [7] M. Benedetti, E. Lloyd, S. Sack, and M. Fiorentini, Parameterized quantum circuits as machine learning models, *Quantum Science and Technology* **4**, 043001 (2019).
- [8] S. Jerbi, L. J. Fiderer, H. Poulsen Nautrup, J. M. Kübler, H. J. Briegel, and V. Dunjko, Quantum machine learning beyond kernel methods, *Nature Communications* **14**, 517 (2023).
- [9] M. Cerezo, A. Arrasmith, R. Babbush, S. C. Benjamin, S. Endo, K. Fujii, J. R. McClean, K. Mitarai, X. Yuan, L. Cincio, and P. J. Coles, Variational quantum algorithms, *Nature Reviews Physics* **3**, 625 (2021).
- [10] N. Moll, P. Barkoutsos, L. S. Bishop, J. M. Chow, A. Cross, D. J. Egger, S. Filipp, A. Fuhrer, J. M. Gambetta, M. Ganzhorn, A. Kandala, A. Mezzacapo, P. Müller, W. Riess, G. Salis, J. Smolin, I. Tavernelli, and K. Temme, Quantum optimization using variational algorithms on near-term quantum devices, *Quantum Science and Technology* **3**, 030503 (2018).
- [11] A. Peruzzo, J. McClean, P. Shadbolt, M.-H. Yung, X.-Q. Zhou, P. J. Love, A. Aspuru-Guzik, and J. L. O’Brien, A variational eigenvalue solver on a photonic quantum processor, *Nature Communications* **5**, 4213 (2014).
- [12] L. Zhou, S.-T. Wang, S. Choi, H. Pichler, and M. D. Lukin, Quantum approximate optimization algorithm: Performance, mechanism, and implementation on near-term devices, *Phys. Rev. X* **10**, 021067 (2020).
- [13] C. Tabares, A. Muñoz de las Heras, L. Tagliacozzo, D. Porras, and A. González-Tudela, Variational quantum simulators based on waveguide qed, *Phys. Rev. Lett.* **131**, 073602 (2023).
- [14] X. Pan, Z. Lu, W. Wang, Z. Hua, Y. Xu, W. Li, W. Cai, X. Li, H. Wang, Y.-P. Song, C.-L. Zou, D.-L. Deng, and L. Sun, Deep quantum neural networks on a superconducting processor, *Nature Communications* **14**, 4006 (2023).
- [15] S. McArdle, S. Endo, A. Aspuru-Guzik, S. C. Benjamin, and X. Yuan, Quantum computational chemistry, *Rev. Mod. Phys.* **92**, 015003 (2020).
- [16] A. Kandala, A. Mezzacapo, K. Temme, M. Takita, M. Brink, J. M. Chow, and J. M. Gambetta, Hardware-efficient variational quantum eigensolver for small molecules and quantum magnets, *Nature* **549**, 242 (2017).
- [17] C. Hempel, C. Maier, J. Romero, J. McClean, T. Monz, H. Shen, P. Jurcevic, B. P. Lanyon, P. Love, R. Babbush, A. Aspuru-Guzik, R. Blatt, and C. F. Roos, Quantum chemistry calculations on a trapped-ion quantum simulator, *Phys. Rev. X* **8**, 031022 (2018).
- [18] D. Amaro, C. Modica, M. Rosenkranz, M. Fiorentini, M. Benedetti, and M. Lubasch, Filtering variational quantum algorithms for combinatorial optimization, *Quantum Science and Technology* **7**, 015021 (2022).
- [19] V. Akshay, H. Philathong, M. E. S. Morales, and J. D. Biamente, Reachability deficits in quantum approximate optimization, *Phys. Rev. Lett.* **124**, 090504 (2020).
- [20] V. Havlíček, A. D. Córcoles, K. Temme, A. W. Harrow, A. Kandala, J. M. Chow, and J. M. Gambetta, Supervised learning with quantum-enhanced feature spaces, *Nature* **567**, 209 (2019).
- [21] V. Saggio, B. E. Asenbeck, A. Hamann, T. Strömberg, P. Schiavsky, V. Dunjko, N. Friis, N. C. Harris, M. Hochberg, D. Englund, S. Wölk, H. J. Briegel, and P. Walther, Experimental quantum speed-up in reinforcement learning agents, *Nature* **591**, 229 (2021).
- [22] M. Schuld, A. Bocharov, K. M. Svore, and N. Wiebe, Circuit-centric quantum classifiers, *Phys. Rev. A* **101**, 032308 (2020).
- [23] M. Schuld and N. Killoran, Quantum machine learning in feature hilbert spaces, *Phys. Rev. Lett.* **122**, 040504 (2019).
- [24] R. Sweke, F. Wilde, J. Meyer, M. Schuld, P. K. Faehrmann, B. Meynard-Piganeau, and J. Eisert, Stochastic gradient descent for hybrid quantum-classical optimization, *Quantum* **4**, 314 (2020).
- [25] A. Basheer, Y. Feng, C. Ferrie, and S. Li, Alternating layered variational quantum circuits can be classically optimized efficiently using classical shadows, in *Proceedings of the AAAI Conference on Artificial Intelligence*, Vol. 37 (2023) pp. 6770–6778.
- [26] J. A. Nelder and R. Mead, A simplex method for function minimization, *Computer Journal* **7**, 308 (1965).
- [27] M. J. Powell, An efficient method for finding the minimum of a function of several variables without calculating derivatives, *The computer journal* **7**, 155 (1964).

- [28] J. R. McClean, S. Boixo, V. N. Smelyanskiy, R. Babbush, and H. Neven, Barren plateaus in quantum neural network training landscapes, *Nature Communications* **9**, 4812 (2018).
- [29] A. Arrasmith, M. Cerezo, P. Czarnik, L. Cincio, and P. J. Coles, Effect of barren plateaus on gradient-free optimization, *Quantum* **5**, 558 (2021).
- [30] Z. Liu, L.-W. Yu, L.-M. Duan, and D.-L. Deng, Presence and absence of barren plateaus in tensor-network based machine learning, *Phys. Rev. Lett.* **129**, 270501 (2022).
- [31] C. Ortiz Marrero, M. Kieferová, and N. Wiebe, Entanglement-induced barren plateaus, *PRX Quantum* **2**, 040316 (2021).
- [32] K. Zhang, L. Liu, M.-H. Hsieh, and D. Tao, Escaping from the barren plateau via gaussian initializations in deep variational quantum circuits, in *Advances in Neural Information Processing Systems*, edited by A. H. Oh, A. Agarwal, D. Belgrave, and K. Cho (2022).
- [33] Y. Wang, B. Qi, C. Ferrie, and D. Dong, Trainability enhancement of parameterized quantum circuits via reduced-domain parameter initialization, arXiv preprint arXiv:2302.06858 (2023).
- [34] L. Friedrich and J. Maziero, Avoiding barren plateaus with classical deep neural networks, *Phys. Rev. A* **106**, 042433 (2022).
- [35] H.-Y. Liu, T.-P. Sun, Y.-C. Wu, Y.-J. Han, and G.-P. Guo, Mitigating barren plateaus with transfer-learning-inspired parameter initializations, *New Journal of Physics* **25**, 013039 (2023).
- [36] C. Zhao and X.-S. Gao, Analyzing the barren plateau phenomenon in training quantum neural networks with the ZX-calculus, *Quantum* **5**, 466 (2021).
- [37] A. Pesah, M. Cerezo, S. Wang, T. Volkoff, A. T. Sornborger, and P. J. Coles, Absence of barren plateaus in quantum convolutional neural networks, *Phys. Rev. X* **11**, 041011 (2021).
- [38] I. Cong, S. Choi, and M. D. Lukin, Quantum convolutional neural networks, *Nature Physics* **15**, 1273 (2019).
- [39] A. G. Taube and R. J. Bartlett, New perspectives on unitary coupled-cluster theory, *International Journal of Quantum Chemistry* **106**, 3393 (2006), <https://onlinelibrary.wiley.com/doi/pdf/10.1002/qua.21198>.
- [40] D. Wecker, M. B. Hastings, and M. Troyer, Progress towards practical quantum variational algorithms, *Phys. Rev. A* **92**, 042303 (2015).
- [41] S.-X. Zhang, Z.-Q. Wan, C.-K. Lee, C.-Y. Hsieh, S. Zhang, and H. Yao, Variational quantum-neural hybrid eigensolver, *Phys. Rev. Lett.* **128**, 120502 (2022).
- [42] P. J. J. O'Malley, R. Babbush, I. D. Kivlichan, J. Romero, J. R. McClean, R. Barends, J. Kelly, P. Roushan, A. Tranter, N. Ding, B. Campbell, Y. Chen, Z. Chen, B. Chiaro, A. Dunsworth, A. G. Fowler, E. Jeffrey, E. Lucero, A. Megrant, J. Y. Mutus, M. Neeley, C. Neill, C. Quintana, D. Sank, A. Vainsencher, J. Wenner, T. C. White, P. V. Coveney, P. J. Love, H. Neven, A. Aspuru-Guzik, and J. M. Martinis, Scalable quantum simulation of molecular energies, *Phys. Rev. X* **6**, 031007 (2016).
- [43] D. Reynolds, Gaussian mixture models, in *Encyclopedia of Biometrics*, edited by S. Z. Li and A. K. Jain (Springer US, Boston, MA, 2015) pp. 827–832.
- [44] C. Rasmussen, The infinite gaussian mixture model, in *Advances in Neural Information Processing Systems*, Vol. 12, edited by S. Solla, T. Leen, and K. Müller (MIT Press, 1999).
- [45] G. Xuan, W. Zhang, and P. Chai, EM algorithms of gaussian mixture model and hidden markov model, in *Proceedings 2001 International Conference on Image Processing (Cat. No. 01CH37205)*, Vol. 1 (2001) pp. 145–148 vol.1.
- [46] B. Zong, Q. Song, M. R. Min, W. Cheng, C. Lumezanu, D. Cho, and H. Chen, Deep autoencoding gaussian mixture model for unsupervised anomaly detection, in *International Conference on Learning Representations* (2018).
- [47] M.-S. Yang, C.-Y. Lai, and C.-Y. Lin, A robust EM clustering algorithm for gaussian mixture models, *Pattern Recognition* **45**, 3950 (2012).
- [48] L. Manduchi, K. Chin-Cheong, H. Michel, S. Wellmann, and J. E. Vogt, Deep conditional gaussian mixture model for constrained clustering, in *Advances in Neural Information Processing Systems*, edited by A. Beygelzimer, Y. Dauphin, P. Liang, and J. W. Vaughan (2021).
- [49] M. Glodek, M. Schels, and F. Schwenker, Ensemble gaussian mixture models for probability density estimation, *Computational Statistics* **28**, 127 (2013).
- [50] H. GM, M. K. Gourisaria, M. Pandey, and S. S. Rautaray, A comprehensive survey and analysis of generative models in machine learning, *Computer Science Review* **38**, 100285 (2020).
- [51] K. Sharma, M. Cerezo, L. Cincio, and P. J. Coles, Trainability of dissipative perceptron-based quantum neural networks, *Phys. Rev. Lett.* **128**, 180505 (2022).
- [52] M. Cerezo, A. Sone, T. Volkoff, L. Cincio, and P. J. Coles, Cost function dependent barren plateaus in shallow parametrized quantum circuits, *Nature Communications* **12**, 1791 (2021).
- [53] See Supplemental Material for details on proofs of Theorem 1, 2 and 3, also with the numerical simulations details.
- [54] K. Bharti and T. Haug, Iterative quantum-assisted eigensolver, *Phys. Rev. A* **104**, L050401 (2021).
- [55] J. Romero, J. P. Olson, and A. Aspuru-Guzik, Quantum autoencoders for efficient compression of quantum data, *Quantum Science and Technology* **2**, 045001 (2017).
- [56] J. Biamonte, P. Wittek, N. Pancotti, P. Rebentrost, N. Wiebe, and S. Lloyd, Quantum machine learning, *Nature* **549**, 195 (2017).
- [57] I. S. Maria Schuld and F. Petruccione, An introduction to quantum machine learning, *Contemporary Physics* **56**, 172 (2015), <https://doi.org/10.1080/00107514.2014.964942>.
- [58] G. A. Quantum, Collaborators*†, F. Arute, K. Arya, R. Babbush, D. Bacon, J. C. Bardin, R. Barends, S. Boixo, M. Broughton, B. B. Buckley, D. A. Buell, B. Burkett, N. Bushnell, Y. Chen, Z. Chen, B. Chiaro, R. Collins, W. Courtney, S. Demura, A. Dunsworth, E. Farhi, A. Fowler, B. Foxen, C. Gidney, M. Giustina, R. Graff, S. Habegger, M. P. Harrigan, A. Ho, S. Hong, T. Huang, W. J. Huggins, L. Ioffe, S. V. Isakov, E. Jeffrey, Z. Jiang, C. Jones, D. Kafri, K. Kechedzhi, J. Kelly, S. Kim, P. V. Klimov, A. Korotkov, F. Kostritsa, D. Landhuis, P. Laptev, M. Lindmark, E. Lucero, O. Martin, J. M. Martinis, J. R. McClean, M. McEwen, A. Megrant, X. Mi, M. Mohseni, W. Mruczkiewicz, J. Mutus, O. Naaman, M. Neeley, C. Neill, H. Neven, M. Y. Niu, T. E. O'Brien, E. Ostby, A. Petukhov, H. Putterman, C. Quintana, P. Roushan, N. C. Rubin, D. Sank, K. J. Satzinger, V. Smelyanskiy, D. Strain, K. J. Sung, M. Szalay, T. Y. Takeshita, A. Vainsencher, T. White, N. Wiebe, Z. J. Yao, P. Yeh, and A. Zalcman, Hartree-fock on a superconducting qubit quantum computer, *Science* **369**, 1084 (2020), <https://www.science.org/doi/pdf/10.1126/science.abb9811>.
- [59] I. N. Levine, D. H. Busch, and H. Shull, *Quantum chemistry*, Vol. 6 (Pearson Prentice Hall Upper Saddle River, NJ, 2009).
- [60] Y. Cao, J. Romero, J. P. Olson, M. Degroote, P. D. Johnson, M. Kieferová, I. D. Kivlichan, T. Menke, B. Peropadre, N. P. D. Sawaya, S. Sim, L. Veis, and A. Aspuru-Guzik, Quantum chemistry in the age of quantum computing, *Chemical Reviews* **119**, 10856 (2019).
- [61] R. B. Stinchcombe, Ising model in a transverse field. i. basic theory, *Journal of Physics C: Solid State Physics* **6**, 2459 (1973).
- [62] M. Heyl, A. Polkovnikov, and S. Kehrein, Dynamical quantum

- phase transitions in the transverse-field ising model, *Phys. Rev. Lett.* **110**, 135704 (2013).
- [63] X. Shi, Github repository, <https://github.com/iwrache/GMM-BP>.
- [64] R. J. Garcia, C. Zhao, K. Bu, and A. Jaffe, Barren plateaus from learning scramblers with local cost functions, *Journal of High Energy Physics* **2023**, 90 (2023).
- [65] L. Bittel and M. Kliesch, Training variational quantum algorithms is np-hard, *Phys. Rev. Lett.* **127**, 120502 (2021).
- [66] E. R. Anschuetz and B. T. Kiani, Quantum variational algorithms are swamped with traps, *Nature Communications* **13**, 7760 (2022).

SUPPLEMENTAL MATERIALS

PRELIMINARIES

For the sake of convenience, let's introduce some notations. If there are two observables $O_i = o_1^i \otimes o_2^i \otimes \dots \otimes o_N^i$ and $O_j = o_1^j \otimes o_2^j \otimes \dots \otimes o_N^j$, $\forall l \in [N]$, the single observables o_l^i and o_l^j at their corresponding positions belong to the set $\{X, X; Y, Y; Z, Z; I, Z; Z, I; I, I\}$. We define:

$$S_1^{ij} := |\{m | o_m^i = o_m^j = X, m \in [N]\}| \quad (\text{S1})$$

$$P_0^{ij} := \{m | o_m^i = I | o_m^j = I, m \in [N]\} \quad (\text{S2})$$

$$P_{1:3}^{ij} := \{m | o_m^i = o_m^j \neq I, m \in [N]\} \quad (\text{S3})$$

$$(\text{S4})$$

Also, the random variable θ is distributed according to $\mathcal{G}_0, \mathcal{G}_1(\sigma^2), \mathcal{G}_2(\sigma^2), \mathcal{G}_3(\sigma^2)$, adhering to the same definitions as presented in the main text. Assuming θ follows the distribution $\mathcal{G}_1(\sigma^2)$, we define α, β , and γ as follows:

$$\alpha = \mathbb{E}_{\theta \sim \mathcal{G}_1(\sigma^2)} \cos^2 \theta = \frac{1 + e^{-2\sigma^2}}{2} \quad (\text{S5})$$

$$\beta = \mathbb{E}_{\theta \sim \mathcal{G}_1(\sigma^2)} \sin^2 \theta = \frac{1 - e^{-2\sigma^2}}{2} \quad (\text{S6})$$

$$\gamma = \mathbb{E}_{\theta \sim \mathcal{G}_1(\sigma^2)} \cos \theta = e^{-\frac{\sigma^2}{2}} \quad (\text{S7})$$

By straightforward application of a Taylor expansion, it is evident that $\alpha \geq 1 - \sigma^2$ and $\beta \geq \sigma^2(1 - \sigma^2)$.

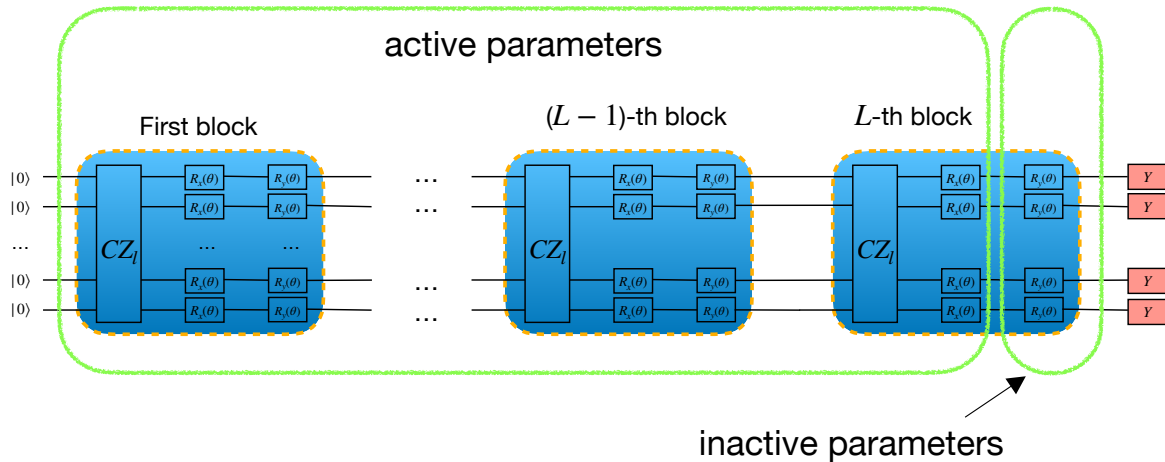


FIG. S1. When a term in the observable is Y , the parameters in the last block's $R_y(\theta)$ in the ansatz do not contribute to the training. Moreover, when the entire observable consists of Y , the θ parameters in the R_y gates of the last block have no impact on the cost function.

We will now delve into the relationship between observables and inactive parameters. Let's assume the observable \mathbf{O} is a global observable, i.e., $\mathbf{O} = o_1 \otimes o_2 \otimes \dots \otimes o_N$, where $\forall k \in \{1, 2, \dots, N\}, o_k \in \{X, Y, Z\}$. Let the density matrix of the final quantum state be ρ_{2L} , and the quantum state just before the final R_y rotation gate in the last block be ρ_{2L-1} . We find that

$f(\theta) = \text{Tr}[\mathbf{O}\rho_{2L}] = \text{Tr}[\mathbf{O}(R_y(\theta_{2L,1}) \otimes R_y(\theta_{2L,2}) \otimes \dots \otimes R_y(\theta_{2L,N}))\rho_{2L-1}(R_y^\dagger(\theta_{2L,1}) \otimes R_y^\dagger(\theta_{2L,2}) \otimes \dots \otimes R_y^\dagger(\theta_{2L,N}))]$. Then, when $o_k = Y$, we notice that $\forall \theta_{2L,k}, R_y(\theta_{2L,k})YR_y^\dagger(\theta_{2L,k}) = Y$. Obviously, in this case, $\theta_{2L,k}$ is independent of the cost function $f(\theta)$, making it an "inactive parameter." When the observable $\mathbf{O} = Y \otimes Y \otimes \dots \otimes Y$, as shown in Fig. S1, all parameters in the last layer of R_y gates are inactive parameters.

TECHNICAL LEMMAS

Lemma 1. *Let ρ be an arbitrary linear operator; G be a Hermitian unitary and $V = e^{-i\frac{\theta}{2}G}$. Consider an arbitrary Hamiltonian operator O that commutes with G . Moreover, let θ be a random variable following an arbitrary distribution, i.e., $\theta \sim \mathcal{G}_0$. Then:*

$$\mathbb{E}_{\theta \sim \mathcal{G}_0} \text{Tr}[OV\rho V^\dagger] = \text{Tr}[O\rho] \quad (\text{S8})$$

$$\mathbb{E}_{\theta \sim \mathcal{G}_0} \text{Tr}^2[OV\rho V^\dagger] = \text{Tr}^2[O\rho] \quad (\text{S9})$$

$$\mathbb{E}_{\theta \sim \mathcal{G}_0} \frac{\partial}{\partial \theta} \text{Tr}[OV\rho V^\dagger] = 0 \quad (\text{S10})$$

where $\text{Tr}^2[\cdot] = (\text{Tr}[\cdot])^2$

Proof. Consider that $V = e^{-i\frac{\theta}{2}G} = I \cos\left(\frac{\theta}{2}\right) - iG \sin\left(\frac{\theta}{2}\right)$, for any arbitrary operator O , we obtain:

$$\begin{aligned} \text{Tr}[OV\rho V^\dagger] &= \text{Tr}\left[O\left(I \cos\left(\frac{\theta}{2}\right) - iG \sin\left(\frac{\theta}{2}\right)\right)\rho\left(I \cos\left(\frac{\theta}{2}\right) + iG \sin\left(\frac{\theta}{2}\right)\right)\right] \\ &= \frac{1+\cos\theta}{2}\text{Tr}[O\rho] + \frac{1-\cos\theta}{2}\text{Tr}[OG\rho G] + \frac{\sin\theta}{2}(\text{Tr}[iO\rho G] - \text{Tr}[iOG\rho]) \end{aligned} \quad (\text{S11})$$

Given that G is unitary and $[O, G] = 0$, the above expression simplifies to:

$$\text{Tr}[OV\rho V^\dagger] = \text{Tr}[O\rho] \quad (\text{S12})$$

Hence, $\text{Tr}[OV\rho V^\dagger]$ is independent of θ . Consequently, for any random variable θ , we establish that $\mathbb{E}_{\theta \sim \mathcal{G}_0} \text{Tr}[OV\rho V^\dagger] = \text{Tr}[O\rho]$, $\mathbb{E}_{\theta \sim \mathcal{G}_0} \text{Tr}^2[OV\rho V^\dagger] = \text{Tr}^2[O\rho]$ and $\mathbb{E}_{\theta \sim \mathcal{G}_0} \frac{\partial}{\partial \theta} \text{Tr}[OV\rho V^\dagger] = 0$.

Lemma 2. *Let ρ be an arbitrary linear operator, and let G be a Hermitian unitary and $V = e^{-i\frac{\theta}{2}G}$. Consider arbitrary Hamiltonian operator O_1, O_2, \tilde{O}_1 , and \tilde{O}_2 , where O_1, O_2 anti-commute with G and \tilde{O}_1, \tilde{O}_2 commute with G , implying $\{O_1, G\} = 0, \{O_2, G\} = 0, [\tilde{O}_1, G] = 0$, and $[\tilde{O}_2, G] = 0$. And θ is a random variable following a Gaussian distribution $\mathcal{N}(0, \sigma^2)$, i.e., $\theta \sim \mathcal{G}_1(\sigma^2)$. Then:*

$$\mathbb{E}_{\theta \sim \mathcal{G}_1(\sigma^2)} \text{Tr}[O_1 V \rho V^\dagger] = \gamma \text{Tr}[O_1 \rho] \quad (\text{S13})$$

$$\mathbb{E}_{\theta \sim \mathcal{G}_1(\sigma^2)} \frac{\partial}{\partial \theta} \text{Tr}[O_1 V \rho V^\dagger] = \gamma \text{Tr}[iGO_1 \rho] \quad (\text{S14})$$

$$\mathbb{E}_{\theta \sim \mathcal{G}_1(\sigma^2)} \text{Tr}[\tilde{O}_1 V \rho V^\dagger] \text{Tr}[O_1 V \rho V^\dagger] = \gamma \text{Tr}[\tilde{O}_1 \rho] \text{Tr}[O_1 \rho] \quad (\text{S15})$$

$$\mathbb{E}_{\theta \sim \mathcal{G}_1(\sigma^2)} \frac{\partial}{\partial \theta} \text{Tr}[\tilde{O}_1 V \rho V^\dagger] \frac{\partial}{\partial \theta} \text{Tr}[O_2 V \rho V^\dagger] = \mathbb{E}_{\theta \sim \mathcal{G}_1(\sigma^2)} \frac{\partial}{\partial \theta} \text{Tr}[\tilde{O}_1 V \rho V^\dagger] \frac{\partial}{\partial \theta} \text{Tr}[\tilde{O}_2 V \rho V^\dagger] = 0 \quad (\text{S16})$$

$$\mathbb{E}_{\theta \sim \mathcal{G}_1(\sigma^2)} \text{Tr}[O_1 V \rho V^\dagger] \text{Tr}[O_2 V \rho V^\dagger] = \alpha \text{Tr}[O_1 \rho] \text{Tr}[O_2 \rho] + \beta \text{Tr}[iGO_1 \rho] \text{Tr}[iGO_2 \rho] \quad (\text{S17})$$

$$\mathbb{E}_{\theta \sim \mathcal{G}_1(\sigma^2)} \frac{\partial}{\partial \theta} \text{Tr}[O_1 V \rho V^\dagger] \frac{\partial}{\partial \theta} \text{Tr}[O_2 V \rho V^\dagger] = \beta \text{Tr}[O_1 \rho] \text{Tr}[O_2 \rho] + \alpha \text{Tr}[iGO_1 \rho] \text{Tr}[iGO_2 \rho] \quad (\text{S18})$$

where i is the imaginary unit.

proof. According to Eq. (S11), it can be seen that for any operator O , we have

$$\text{Tr}[OV \rho V^\dagger] = \frac{1+\cos \theta}{2} \text{Tr}[O \rho] + \frac{1-\cos \theta}{2} \text{Tr}[GOG \rho] + \frac{\sin \theta}{2} (\text{Tr}[iGO \rho] - \text{Tr}[iOG \rho]) \quad (\text{S19})$$

Considering the unitarity of G and the conditions $\{O_1, G\} = 0$, as indicated in Eq. (S19), we can deduce that

$$\text{Tr}[O_1 V \rho V^\dagger] = \cos \theta \text{Tr}[O_1 \rho] + \sin \theta \text{Tr}[iGO_1 \rho] \quad (\text{S20})$$

Based on Eq. (S20), we obtain that

$$\frac{\partial}{\partial \theta} \text{Tr}[O_1 V \rho V^\dagger] = -\sin \theta \text{Tr}[O_1 \rho] + \cos \theta \text{Tr}[iGO_1 \rho] \quad (\text{S21})$$

Given that $\mathbb{E}_{\theta \sim \mathcal{G}_1(\sigma^2)} \sin \theta = \mathbb{E}_{\theta \sim \mathcal{G}_1(\sigma^2)} \sin 2\theta = 0$, and combining it with Eq. (S12), Eq. (S20) and Eq. (S21). Therefore, we can deduce Eq. (S13) to Eq. (S18).

Lemma 3. Let ρ , G , V , O_1 , O_2 , \tilde{O}_1 and \tilde{O}_2 be defined in the same manner as presented in Lemma 2. Random variable θ follows distribution $\mathcal{G}_2(\sigma^2)$. Then

$$\mathbb{E}_{\theta \sim \mathcal{G}_2(\sigma^2)} \text{Tr}[O_1 V \rho V^\dagger] = 0 \quad (\text{S22})$$

$$\mathbb{E}_{\theta \sim \mathcal{G}_2(\sigma^2)} \frac{\partial}{\partial \theta} \text{Tr}[O_1 V \rho V^\dagger] = 0 \quad (\text{S23})$$

$$\mathbb{E}_{\theta \sim \mathcal{G}_2(\sigma^2)} \text{Tr}[\tilde{O}_1 V \rho V^\dagger] \text{Tr}[O_1 V \rho V^\dagger] = 0 \quad (\text{S24})$$

$$\mathbb{E}_{\theta \sim \mathcal{G}_2(\sigma^2)} \text{Tr}[\tilde{O}_1 V \rho V^\dagger] \text{Tr}[\tilde{O}_2 V \rho V^\dagger] = \text{Tr}[\tilde{O}_1 \rho] \text{Tr}[\tilde{O}_2 \rho] \quad (\text{S25})$$

$$\mathbb{E}_{\theta \sim \mathcal{G}_2(\sigma^2)} \frac{\partial}{\partial \theta} \text{Tr}[\tilde{O}_1 V \rho V^\dagger] \frac{\partial}{\partial \theta} \text{Tr}[O_2 V \rho V^\dagger] = \mathbb{E}_{\theta \sim \mathcal{G}_2(\sigma^2)} \frac{\partial}{\partial \theta} \text{Tr}[\tilde{O}_1 V \rho V^\dagger] \frac{\partial}{\partial \theta} \text{Tr}[\tilde{O}_2 V \rho V^\dagger] = 0 \quad (\text{S26})$$

$$\mathbb{E}_{\theta \sim \mathcal{G}_2(\sigma^2)} \text{Tr}[O_1 V \rho V^\dagger] \text{Tr}[O_2 V \rho V^\dagger] = \beta \text{Tr}[O_1 \rho] \text{Tr}[O_2 \rho] + \alpha \text{Tr}[iGO_1 \rho] \text{Tr}[iGO_2 \rho] \quad (\text{S27})$$

$$\mathbb{E}_{\theta \sim \mathcal{G}_2(\sigma^2)} \frac{\partial}{\partial \theta} \text{Tr}[O_1 V \rho V^\dagger] \frac{\partial}{\partial \theta} \text{Tr}[O_2 V \rho V^\dagger] = \alpha \text{Tr}[O_1 \rho] \text{Tr}[O_2 \rho] + \beta \text{Tr}[i G O_1 \rho] \text{Tr}[i G O_2 \rho] \quad (\text{S28})$$

proof. Since $\theta \sim \mathcal{G}_2(\sigma^2)$, we have

$$\mathbb{E}_{\theta \sim \mathcal{G}_2(\sigma^2)} \cos \theta = \frac{1}{2} \int_{-\infty}^{+\infty} \frac{1}{\sqrt{2\pi\sigma}} e^{-\frac{(x+\frac{\pi}{2})^2}{2\sigma^2}} \cos(x) dx + \frac{1}{2} \int_{-\infty}^{+\infty} \frac{1}{\sqrt{2\pi\sigma}} e^{-\frac{(x-\frac{\pi}{2})^2}{2\sigma^2}} \cos(x) dx \quad (\text{S29})$$

$$= -\frac{1}{2} \int_{-\infty}^{+\infty} \frac{1}{\sqrt{2\pi\sigma}} e^{-\frac{x^2}{2\sigma^2}} \sin(x) dx + \frac{1}{2} \int_{-\infty}^{+\infty} \frac{1}{\sqrt{2\pi\sigma}} e^{-\frac{x^2}{2\sigma^2}} \sin(x) dx \quad (\text{S30})$$

$$= 0 \quad (\text{S31})$$

By following the similar calculations, we obtain $\mathbb{E}_{\theta \sim \mathcal{G}_2(\sigma^2)} \sin(2\theta) = 0$, $\mathbb{E}_{\theta \sim \mathcal{G}_2(\sigma^2)} \cos^2(\theta) = \beta$, $\mathbb{E}_{\theta \sim \mathcal{G}_2(\sigma^2)} \sin^2(\theta) = \alpha$. Combining them with Eq. (S12) and Eq. (S20), it is straightforward to have Eq. (S22) to Eq. (S28).

Lemma 4. *The definitions of ρ , G , V , O_1 , O_2 , \tilde{O}_1 and \tilde{O}_2 align with those outlined in Lemma 2. Random variable θ follows distribution $\mathcal{G}_3(\sigma^2)$. Then*

$$\mathbb{E}_{\theta \sim \mathcal{G}_3(\sigma^2)} \text{Tr}[O_1 V \rho V^\dagger] = 0 \quad (\text{S32})$$

$$\mathbb{E}_{\theta \sim \mathcal{G}_3(\sigma^2)} \frac{\partial}{\partial \theta} \text{Tr}[O_1 V \rho V^\dagger] = 0 \quad (\text{S33})$$

$$\mathbb{E}_{\theta \sim \mathcal{G}_3(\sigma^2)} \text{Tr}[\tilde{O}_1 V \rho V^\dagger] \text{Tr}[O_1 V \rho V^\dagger] = 0 \quad (\text{S34})$$

$$\mathbb{E}_{\theta \sim \mathcal{G}_3(\sigma^2)} \text{Tr}[\tilde{O}_1 V \rho V^\dagger] \text{Tr}[\tilde{O}_2 V \rho V^\dagger] = \text{Tr}[\tilde{O}_1 \rho] \text{Tr}[\tilde{O}_2 \rho] \quad (\text{S35})$$

$$\mathbb{E}_{\theta \sim \mathcal{G}_3(\sigma^2)} \frac{\partial}{\partial \theta} \text{Tr}[\tilde{O}_1 V \rho V^\dagger] \frac{\partial}{\partial \theta} \text{Tr}[O_2 V \rho V^\dagger] = \mathbb{E}_{\theta} \frac{\partial}{\partial \theta} \text{Tr}[\tilde{O}_1 V \rho V^\dagger] \frac{\partial}{\partial \theta} \text{Tr}[\tilde{O}_2 V \rho V^\dagger] = 0 \quad (\text{S36})$$

$$\mathbb{E}_{\theta \sim \mathcal{G}_3(\sigma^2)} \text{Tr}[O_1 V \rho V^\dagger] \text{Tr}[O_2 V \rho V^\dagger] = \alpha \text{Tr}[O_1 \rho] \text{Tr}[O_2 \rho] + \beta \text{Tr}[i G O_1 \rho] \text{Tr}[i G O_2 \rho] \quad (\text{S37})$$

$$\mathbb{E}_{\theta \sim \mathcal{G}_3(\sigma^2)} \frac{\partial}{\partial \theta} \text{Tr}[O_1 V \rho V^\dagger] \frac{\partial}{\partial \theta} \text{Tr}[O_2 V \rho V^\dagger] = \beta \text{Tr}[O_1 \rho] \text{Tr}[O_2 \rho] + \alpha \text{Tr}[i G O_1 \rho] \text{Tr}[i G O_2 \rho] \quad (\text{S38})$$

proof. Since $\theta \sim \mathcal{G}_3(\sigma^2)$, we have

$$\mathbb{E}_{\theta \sim \mathcal{G}_3(\sigma^2)} \cos \theta = \frac{1}{4} \int_{-\infty}^{+\infty} \frac{1}{\sqrt{2\pi\sigma}} e^{-\frac{(x+\pi)^2}{2\sigma^2}} \cos(x) dx + \frac{1}{4} \int_{-\infty}^{+\infty} \frac{1}{\sqrt{2\pi\sigma}} e^{-\frac{(x-\pi)^2}{2\sigma^2}} \cos(x) dx + \frac{1}{2} \int_{-\infty}^{+\infty} \frac{1}{\sqrt{2\pi\sigma}} e^{-\frac{x^2}{2\sigma^2}} \cos(x) dx \quad (\text{S39})$$

$$= -\frac{1}{4} \int_{-\infty}^{+\infty} \frac{1}{\sqrt{2\pi\sigma}} e^{-\frac{x^2}{2\sigma^2}} \cos(x) dx - \frac{1}{4} \int_{-\infty}^{+\infty} \frac{1}{\sqrt{2\pi\sigma}} e^{-\frac{x^2}{2\sigma^2}} \cos(x) dx + \frac{1}{2} \int_{-\infty}^{+\infty} \frac{1}{\sqrt{2\pi\sigma}} e^{-\frac{x^2}{2\sigma^2}} \cos(x) dx \quad (\text{S40})$$

$$= 0 \quad (\text{S41})$$

By following the similar calculations, we obtain $\mathbb{E}_\theta \sin(2\theta) = 0$, $\mathbb{E}_\theta \cos^2(\theta) = \alpha$, $\mathbb{E}_\theta \sin^2(\theta) = \beta$. Again using Eq. (S12) and Eq. (S20), it is straightforward to have Eq. (S32) to Eq. (S38).

When $O_1 = O_2$ and $\tilde{O}_1 = \tilde{O}_2$, we can derive the following corollary:

Corollary: *Let ρ be an arbitrary linear operator, and let G be a Hermitian unitary and $V = e^{-i\frac{\theta}{2}G}$. Consider arbitrary quantum observables O , where O anti-commute with G .*

If random variable θ follows distribution $\theta \sim \mathcal{G}_1(\sigma^2)$ or $\theta \sim \mathcal{G}_3(\sigma^2)$. Then

$$\mathbb{E}_\theta \text{Tr}^2[OV\rho V^\dagger] = \alpha \text{Tr}^2[O\rho] + \beta \text{Tr}^2[iGO\rho], \quad (\text{S42})$$

$$\mathbb{E}_\theta \left(\frac{\partial}{\partial \theta} \text{Tr}[OV\rho V^\dagger] \right)^2 = \beta \text{Tr}^2[O\rho] + \alpha \text{Tr}^2[iGO\rho]. \quad (\text{S43})$$

If random variable θ follows a Gaussian mixture model $\theta \sim \mathcal{G}_2(\sigma^2)$. Then

$$\mathbb{E}_\theta \text{Tr}^2[OV\rho V^\dagger] = \beta \text{Tr}^2[O\rho] + \alpha \text{Tr}^2[iGO\rho], \quad (\text{S44})$$

$$\mathbb{E}_\theta \left(\frac{\partial}{\partial \theta} \text{Tr}[OV\rho V^\dagger] \right)^2 = \alpha \text{Tr}^2[O\rho] + \beta \text{Tr}^2[iGO\rho], \quad (\text{S45})$$

For clarity, we employ graphical representations to illustrate the evolution of Pauli matrices. Consider Eq. (S37):

$$\mathbb{E}_{\theta \sim \mathcal{G}_3(\sigma^2)} \text{Tr}[O_1 V \rho V^\dagger] \text{Tr}[O_2 V \rho V^\dagger] = \alpha \text{Tr}[O_1 \rho] \text{Tr}[O_2 \rho] + \beta \text{Tr}[iGO_1 \rho] \text{Tr}[iGO_2 \rho]$$

Suppose $O_1 = X$, $O_2 = Z$, $G = Y$. Then, $iGO_1 = Z$ and $iGO_2 = -X$. Therefore, $\mathbb{E}_{\theta \sim \mathcal{G}_3(\sigma^2)} \text{Tr}[XV\rho V^\dagger] \text{Tr}[ZV\rho V^\dagger] = \alpha \text{Tr}[X\rho] \text{Tr}[Z\rho] - \beta \text{Tr}[Z\rho] \text{Tr}[X\rho]$. The original operators O_1 and O_2 are now split into two terms, XZ and ZX , with coefficients α and $-\beta$ respectively. The corresponding graphical representation, as depicted in Fig. S2, illustrates the evolution of Pauli matrices after applying the gates, with arrows indicating the resulting Pauli matrices and lines representing their parameters.

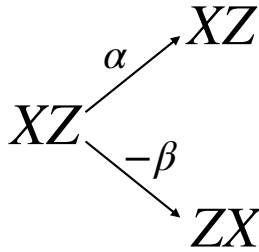


FIG. S2. In the scenario where the density matrix ρ remains invariant, the Pauli matrix XZ undergoes a transformation resulting in two components. One component corresponds to αXZ , while the other corresponds to $-\beta ZX$.

The following lemma pertains to the transformations of 2-qubit Pauli tensor products after the application of a controlled-Z gate.

Lemma 5. *Let CZ represent a controlled-Z gate, and $o_i \otimes o_j$ denote a 2-qubit Pauli tensor product, where o_i and o_j are Pauli matrices. When $o_{i'} \otimes o_{j'}$ is equivalent to $CZ^\dagger(o_i \otimes o_j)CZ$, we denote this transformation as $o_i \otimes o_j \rightarrow o_{i'} \otimes o_{j'}$. To encapsulate all specific transformations succinctly, we present the following summary:*

$$X \otimes I \leftrightarrow X \otimes Z, X \otimes X \leftrightarrow Y \otimes Y, X \otimes Y \leftrightarrow -Y \otimes X, Y \otimes I \leftrightarrow Y \otimes Z$$

$$Y \otimes Z \leftrightarrow Y \otimes I, Z \otimes I \leftrightarrow Z \otimes I, Z \otimes X \leftrightarrow I \otimes X, Z \otimes Y \leftrightarrow I \otimes Y,$$

$$Z \otimes Z \leftrightarrow Z \otimes I, I \otimes I \leftrightarrow I \otimes I, I \otimes Z \leftrightarrow I \otimes Z$$

PROOF OF THEOREM 1

Here, we consider an observable with only one term, i.e. $O = o_1 \otimes o_2 \otimes \dots \otimes o_N$, where $o_i \in \{I, X, Y, Z\}$. For subsequent calculations, we establish the following notations. We define $O_{3:i;1}$ to mean replacing all the Pauli matrices of X in O with Z , and $O_{3:i}$ means replacing all Pauli matrices of X and Y in O with Z . The parameterized quantum circuit $U(\theta)$ comprising L blocks can be represented as

$$U(\theta) = U_L(\theta_{2L}, \theta_{2L-1}) U_{L-1}(\theta_{2L-2}, \theta_{2L-3}) \dots U_1(\theta_2, \theta_1) \quad (\text{S46})$$

For each block $U(\theta_l)$, it can be represented as

$$U_l(\theta_{2l}, \theta_{2l-1}) = R_{2l}(\theta_{2l}) R_{2l-1}(\theta_{2l-1}) CZ_l \quad (\text{S47})$$

where

$$R_{2l}(\theta_{2l}) = e^{-i \frac{\theta_{2l,1}}{2} Y} \otimes e^{-i \frac{\theta_{2l,2}}{2} Y} \dots \otimes e^{-i \frac{\theta_{2l,N}}{2} Y} \quad (\text{S48})$$

$$R_{2l-1}(\theta_{2l-1}) = e^{-i \frac{\theta_{2l-1,1}}{2} X} \otimes e^{-i \frac{\theta_{2l-1,2}}{2} X} \dots \otimes e^{-i \frac{\theta_{2l-1,N}}{2} X}, \quad (\text{S49})$$

CZ_l denotes that the circuit induces entanglement through the inclusion of multiple CZ gates in the l -th block.

Next, we consider the intermediate state. For any $k \in \{0, 1, \dots, 2L\}$, assuming that the quantum state obtained after passing through the k -th block is ρ_k , we define

$$\rho_k := \begin{cases} R_k(\theta_k) \rho_{k-1} R_k(\theta_k)^\dagger & \text{for } k = 2l \leq 2L \\ R_k(\theta_k) CZ_{\frac{k+1}{2}} \rho_{k-1} CZ_{\frac{k+1}{2}}^\dagger R_k(\theta_k)^\dagger & \text{for } k = 2l+1 \leq 2L-1 \end{cases} \quad (\text{S50})$$

Additionally, we define $I_s := \{m | o_m \neq I, m \in [N]\}$ to denote the set of qubits whose observables act nontrivially. Next, we proceed to prove the content of Theorem 1.

Considering the case where $o_i = Z/I$ has two possible choices, namely $\mathcal{G}_1(\sigma^2)$ and $\mathcal{G}_3(\sigma^2)$, we choose $\mathcal{G}_1(\sigma^2)$ without loss of generality. A similar proof can be conducted for the other distribution. First, we consider the expectation of $f(\theta)$. Suppose there exists an index i such that $o_i = X$ or $o_i = Y$. According to Eq.(S22) and Eq. (S23), it is evident that for all q, n , $\mathbb{E}_{\theta} \partial_{\theta_{q,n}} f = 0$.

If the Hamiltonian comprises only Pauli Z and the identity matrix I , and $q = 2L-1$ or $2L$ with $o_n = I$, Eq. (S8) and Eq. (S10) imply $\mathbb{E}_{\theta} \partial_{\theta_{q,n}} f = 0$. When $o_n = Z$, using Eq. (S13) and Eq. (S14), it inevitably transforms into the Pauli matrix X or Y . Combining this with Eq. (S13) and Lemma 5, in the final $\text{Tr}[O' \rho]$, the Pauli matrix at the n -th position of O' must be X or Y . Furthermore, due to $\langle 0|X|0\rangle = \langle 1|X|1\rangle = \langle 0|Y|0\rangle = \langle 1|Y|1\rangle = 0$, we have $\mathbb{E}_{\theta_{[2L]}} \partial_{\theta_{q,n}} \text{Tr}[O \rho_{2L-2}] = 0$. If $q \in \{1, \dots, 2L-2\}$,

then

$$\mathbb{E}_{\theta} \partial_{\theta_{q,n}} f = \mathbb{E}_{\theta_{[2L]}} \partial_{\theta_{q,n}} \text{Tr}[\mathbf{O}\rho_{2L}] \quad (\text{S51})$$

$$= \gamma^{S_3} \mathbb{E}_{\theta_{[2L-1]}} \partial_{\theta_{q,n}} \text{Tr}[\mathbf{O}\rho_{2L-1}] \quad (\text{S52})$$

$$= \gamma^{2S_3} \mathbb{E}_{\theta_{[2L-2]}} \partial_{\theta_{q,n}} \text{Tr}[CZ_l^\dagger \mathbf{O}CZ_l \rho_{2L-2}] \quad (\text{S53})$$

$$= \gamma^{2S_3} \mathbb{E}_{\theta_{[2L-2]}} \partial_{\theta_{q,n}} \text{Tr}[\mathbf{O}\rho_{2L-2}] \quad (\text{S54})$$

$$= \gamma^{(2L-q-1)S_3} \mathbb{E}_{\theta_{[q]}} \partial_{\theta_{q,n}} \text{Tr}[\mathbf{O}\rho_q] \quad (\text{S55})$$

According to Eq. (S8) and (S13), we can infer that when $n \in I_s$, the expectation of θ_n yields γ , and when $n \notin I_s$, the expectation of θ_n results in a constant 1. Thus, we obtain Eq. (S52). Similarly, we can derive Eq. (S53). Eq. (S54) is derived from Lemma 5. By repeating this process, we arrive at Eq. (S55).

We are currently directing our attention to the subscript n . If $n \notin I_S$, then, based on Eq. (S10), we can obtain,

$$\mathbb{E}_{\theta_{[q]}} \partial_{\theta_{q,n}} \text{Tr}[\mathbf{O}\rho_q] = 0 \quad (\text{S56})$$

which means

$$\mathbb{E}_{\theta_{[2L]}} \partial_{\theta_{q,n}} f = 0. \quad (\text{S57})$$

When $n \in I_S$, according to Eq. (S14), we have

$$\mathbb{E}_{\theta_{[q]}} \partial_{\theta_{q,n}} \text{Tr}[\mathbf{O}\rho_{2L-2}] = \gamma^{S_3} \mathbb{E}_{\theta_{[q-1]}} \partial_{\theta_{q,n}} \text{Tr}[\mathbf{O}'\rho_{2L-2}] \quad (\text{S58})$$

Among these, \mathbf{O}' entails transforming the Pauli Z matrix at the n th position of the Hamiltonian \mathbf{O} into Y or $-X$. Subsequently, Eq. (S8) and Eq. (S13) elucidate that applying an expectation to $\theta_1, \theta_2, \dots, \theta_q$ does not alter the form of the observable but merely augments certain coefficients from the previous state. Additionally, considering that the observable at this juncture comprises only Y or $-X$ at the n th position, with the remaining positions being Z or I , Lemma 5 implies that we have

$$\mathbb{E}_{\theta_{[2L]}} \partial_{\theta_{q,n}} \text{Tr}[\mathbf{O}\rho_{2L-2}] = \gamma^c \text{Tr}[\mathbf{O}''\rho_0] \quad (\text{S59})$$

Here, c is a constant greater than or equal to L and less than or equal to $2L$. Considering that the observable \mathbf{O}'' involves the Pauli operators X or Y at position n , and $\langle 0|X|0\rangle = 0$, $\langle 0|Y|0\rangle = 0$, we obtain

$$\mathbb{E}_{\theta_{[2L]}} \partial_{\theta_{q,n}} \text{Tr}[\mathbf{O}\rho_{2L-2}] = 0 \quad (\text{S60})$$

Thus far, we have successfully demonstrated that its expectation is equal to 0. Next, we will establish the lower bound of its gradient norm. Note that

$$\begin{aligned} \mathbb{E}_{\theta} \|\nabla_{\theta} f(\theta)\|^2 &= \sum_{q=1}^{2L} \sum_{n=1}^N \mathbb{E}_{\theta} \left(\frac{\partial f(\theta)}{\partial \theta_{q,n}} \right)^2 \\ &= \sum_{q=1}^{2L} \sum_{n \in I_S} \mathbb{E}_{\theta} \left(\frac{\partial f(\theta)}{\partial \theta_{q,n}} \right)^2 + \sum_{q=1}^{2L} \sum_{n \notin I_S} \mathbb{E}_{\theta} \left(\frac{\partial f(\theta)}{\partial \theta_{q,n}} \right)^2 \\ &\geq \sum_{q=1}^{2L} \sum_{n \in I_S} \mathbb{E}_{\theta} \left(\frac{\partial f(\theta)}{\partial \theta_{q,n}} \right)^2 \end{aligned} \quad (\text{S61})$$

For each term within the first $L-1$ blocks of $\mathbb{E}_{\theta} \left(\frac{\partial f(\theta)}{\partial \theta_{q,n}} \right)^2$, it follows that

$$\mathbb{E}_{\theta} \left(\frac{\partial f(\theta)}{\partial \theta_{q,n}} \right)^2 = \mathbb{E}_{\theta} \left(\frac{\partial}{\partial \theta_{q,n}} \text{Tr}[\mathbf{O}\rho_{2L}] \right)^2 \quad (\text{S62})$$

$$= \mathbb{E}_{\theta_1} \dots \mathbb{E}_{\theta_{2L}} \left(\frac{\partial}{\partial \theta_{q,n}} \text{Tr}[\mathbf{O}R_{2L}(\theta_{2L})\rho_{2L-1}R_{2L}^\dagger(\theta_{2L})] \right)^2 \quad (\text{S63})$$

$$\geq \alpha^{S_1+S_3} \mathbb{E}_{\theta_1} \dots \mathbb{E}_{\theta_{2L-1}} \left(\frac{\partial}{\partial \theta_{q,n}} \text{Tr}[\mathbf{O}_{3:i;1}\rho_{2L-1}] \right)^2 \quad (\text{S64})$$

$$\geq \alpha^{S_1+S_3} \mathbb{E}_{\theta_1} \dots \mathbb{E}_{\theta_{2L-1}} \left(\frac{\partial}{\partial \theta_{q,n}} \text{Tr}[\mathbf{O}_{3:i;1}R_{2L-1}(\theta_{2L-1})CZ_L\rho_{2L-2}CZ_L^\dagger R_{2L}^\dagger(\theta_{2L-1})] \right)^2 \quad (\text{S65})$$

$$\geq \alpha^{S_1+S_3} \alpha^{S_1+S_3+S_2} \mathbb{E}_{\theta_1} \dots \mathbb{E}_{\theta_{2L-2}} \left(\frac{\partial}{\partial \theta_{q,n}} \text{Tr}[\mathbf{O}_{3:i}CZ_L\rho_{2L-2}CZ_L^\dagger] \right)^2 \quad (\text{S66})$$

$$= \alpha^{S_1+S_3} \alpha^{S_1+S_3+S_2} \mathbb{E}_{\theta_1} \dots \mathbb{E}_{\theta_{2L-2}} \left(\frac{\partial}{\partial \theta_{q,n}} \text{Tr}[\mathbf{O}_{3:i}\rho_{2L-2}] \right)^2 \quad (\text{S67})$$

$$\geq \alpha^{S_1+S_3} \alpha^{S(2L-1-q)} \mathbb{E}_{\theta_1} \dots \mathbb{E}_{\theta_q} \left(\frac{\partial}{\partial \theta_{q,n}} \text{Tr}[\mathbf{O}_{3:i}\rho_q] \right)^2 \quad (\text{S68})$$

In Eq. (S64), the formulation arises from the utilization of Eq. (S42) when n is in I_{s_3} and Eq. (S44) when n is in I_{s_1} , contributing a parameter α for each term. Conversely, when n is in either I_{s_0} or I_{s_2} , Eq. (S9) is employed without altering the preceding coefficients. Through analogous analysis, Eq. (S66) is derived. Eq. (S67) is a consequence of the deductions stemming from Lemma 5. By iterating through these steps, we arrive at Eq. (S68).

$$\mathbb{E}_{\theta} \left(\frac{\partial f(\theta)}{\partial \theta_{q,n}} \right)^2 \geq \alpha^{S_1+S_3} \alpha^{S(2L-1-q)} \alpha^{S-1} \beta \mathbb{E}_{\theta_1} \dots \mathbb{E}_{\theta_{q-1}} \left(\text{Tr}[\mathbf{O}_{3:i}\rho_{q-1}] \right)^2 \quad (\text{S69})$$

$$\geq \alpha^{S_1+S_3} \alpha^{S(2L-1-q)} \alpha^{S-1} \beta \alpha^{S(q-1)} \text{Tr}^2[\mathbf{O}_{3:i}\rho_0] \quad (\text{S70})$$

$$\geq \alpha^{2LS-1} \beta \quad (\text{S71})$$

$$\geq (1-\sigma^2)^{2LS-1} \sigma^2 (1-\sigma^2) \quad (\text{S72})$$

$$= \frac{1}{2LS} \left(1 - \frac{1}{2LS}\right)^{2LS} \quad (\text{S73})$$

$$\geq \frac{1}{8LS} \quad (\text{S74})$$

In Eq. (S69), the coefficient β is determined by taking the expectation with respect to $\theta_{q,n}$ based on Eq. (S43). Here, we retain the terms with the coefficient β instead of α . The remaining α^{S-1} terms remain consistent with Eq. (S42). Eq. (S70) follows a process similar to Eq. (S68), obtained by taking the expectation over the remaining θ . Considering $\text{Tr}[\mathbf{O}_{3:i}\rho_0] = 1$, $S_1+S_3 \leq S$, and $\alpha < 1$, we arrive at Eq. (S71). Eq. (S72) is derived from a Taylor expansion. Taking into account $h(x) = (1-\frac{1}{x})^x$ being monotonically increasing when $x \geq 2$, Eq. (S74) is thus proven.

Applying the identical methodology for analysis, we can similarly derive the same results for the R_X rotation layer in the final block. Thus, we can conclude that

$$\begin{aligned} \mathbb{E}_{\theta} \|\nabla_{\theta} f(\theta)\|^2 &\geq \sum_{q=1}^{2L-1} \sum_{n \in I_S} \mathbb{E}_{\theta} \left(\frac{\partial f(\theta)}{\partial \theta_{q,n}} \right)^2 \\ &\geq \sum_{q=1}^{2L-1} \sum_{n \in I_S} \frac{1}{8LS} \\ &= (2L-1) \times S \times \frac{1}{8LS} \\ &= \frac{1}{4} - \frac{1}{8L} \end{aligned} \quad (\text{S75})$$

PROOF OF THEOREM 2

Before proving Theorem 2, let's first consider a special case where both O_i and O_j are global. We can provide the following lemma:

Lemma 6. *Considering a quantum circuit $U(\theta)$ with N qubits, initialized with ρ_0 as a pure state, and employing a hardware-efficient ansatz with L blocks, as depicted in Fig. 1, the cost function is defined as $f(\theta) = \text{Tr}[(\sum_i \mathbf{O}_i - \sum_j \mathbf{O}_j)U(\theta)\rho_0U(\theta)^\dagger]$, where observable $\mathbf{O}_i, \mathbf{O}_j$ are global observables, denoted as $o_i, o_j \in \{X, Y, Z\}$. Randomly choose either \mathbf{O}_i or \mathbf{O}_j and initialize it in accordance with the procedure outlined in Theorem 2. Consequently, we obtain:*

$$\mathbb{E}_\theta \|\nabla_\theta f(\theta)\|_2^2 \geq \frac{1}{4} - \frac{1}{8L} \quad (\text{S76})$$

proof: Without loss of generality, let us opt to specify C_1 and initialize the parameters within $U(\theta)$ following the methodology expounded in Theorem 1. Subsequently, we have

$$\mathbb{E}_\theta \|\nabla_\theta f(\theta)\|_2^2 = \sum_{q,n} \mathbb{E}_\theta \left(\frac{\partial f(\theta)}{\partial \theta_{q,n}} \right)^2 \quad (\text{S77})$$

$$= \sum_{q,n} \mathbb{E}_\theta \left(\sum_i \frac{\partial f_i(\theta)}{\partial \theta_{q,n}} - \sum_j \frac{\partial f_j(\theta)}{\partial \theta_{q,n}} \right)^2 \quad (\text{S78})$$

$$= \sum_{q,n} \mathbb{E}_\theta \left(\sum_i \frac{\partial f_i(\theta)}{\partial \theta_{q,n}} \right)^2 - 2 \sum_{q,n} \mathbb{E}_\theta \left(\sum_{i,j} \frac{\partial f_i(\theta)}{\partial \theta_{q,n}} \cdot \frac{\partial f_j(\theta)}{\partial \theta_{q,n}} \right) + \sum_{q,n} \mathbb{E}_\theta \left(\sum_j \frac{\partial f_j(\theta)}{\partial \theta_{q,n}} \right)^2 \quad (\text{S79})$$

$$= \sum_{q,n,i} \mathbb{E}_\theta \left(\frac{\partial f_i(\theta)}{\partial \theta_{q,n}} \right)^2 + \sum_{q,n,i_1 \neq i_2} \mathbb{E}_\theta \left(\frac{\partial f_{i_1}(\theta)}{\partial \theta_{q,n}} \cdot \frac{\partial f_{i_2}(\theta)}{\partial \theta_{q,n}} \right) - 2 \sum_{q,n,i,j} \mathbb{E}_\theta \left(\frac{\partial f_i(\theta)}{\partial \theta_{q,n}} \cdot \frac{\partial f_j(\theta)}{\partial \theta_{q,n}} \right) + \sum_{q,n,j} \mathbb{E}_\theta \left(\frac{\partial f_j(\theta)}{\partial \theta_{q,n}} \right)^2 + \sum_{q,n,j_1 \neq j_2} \mathbb{E}_\theta \left(\frac{\partial f_{j_1}(\theta)}{\partial \theta_{q,n}} \cdot \frac{\partial f_{j_2}(\theta)}{\partial \theta_{q,n}} \right) \quad (\text{S80})$$

We expand the function $f(\theta)$, resulting in Eq. (S80). Here, $f_i(\theta) = \text{Tr}[\mathbf{O}_i U(\theta)\rho_0 U(\theta)^\dagger]$, $f_j(\theta) = \text{Tr}[\mathbf{O}_j U(\theta)\rho_0 U(\theta)^\dagger]$. Moving forward, let's consider the cross terms. Without loss of generality, let's examine each element in the third term. Let's denote $O_i = \vec{\sigma}_{i,2L} = \sigma_{1,i,2L} \otimes \sigma_{2,i,2L} \otimes \dots \otimes \sigma_{N,i,2L}$ and $O_j = \vec{\sigma}_{j,2L} = \tilde{\sigma}_{1,j,2L} \otimes \tilde{\sigma}_{2,j,2L} \otimes \dots \otimes \tilde{\sigma}_{N,j,2L}$. Next, we focus on the evolution of these Pauli matrices throughout the process, we have:

$$\mathbb{E}_\theta \left(\frac{\partial f_i(\theta)}{\partial \theta} \frac{\partial f_j(\theta)}{\partial \theta} \right) = \mathbb{E}_\theta \left(\frac{\partial}{\partial \theta} \text{Tr}[\vec{\sigma}_{i,2L} \rho_{2L}] \frac{\partial}{\partial \theta} \text{Tr}[\vec{\sigma}_{j,2L} \rho_{2L}] \right) \quad (\text{S81})$$

$$= \mathbb{E}_\theta \left(\frac{\partial}{\partial \theta} \text{Tr}[\vec{\sigma}_{i,2L} R_{2L}(\theta)] \frac{\partial \rho_{2L-1}}{\partial \theta} R_{2L}^\dagger(\theta) \frac{\partial}{\partial \theta} \text{Tr}[\vec{\sigma}_{j,2L} R_{2L}(\theta)] \frac{\partial \rho_{2L-1}}{\partial \theta} R_{2L}^\dagger(\theta) \right) \quad (\text{S82})$$

$$= \sum_{k_1} h_{k_1} \mathbb{E}_\theta \left(\text{Tr}[\vec{\sigma}_{i,2L-1}^{k_1} \frac{\partial \rho_{2L-1}}{\partial \theta}] \text{Tr}[\vec{\sigma}_{j,2L-1}^{k_1} \frac{\partial \rho_{2L-1}}{\partial \theta}] \right) \quad (\text{S83})$$

$$= \sum_{k_2} h_{k_2} \mathbb{E}_\theta \left(\text{Tr}[CZ^\dagger \vec{\sigma}_{i,2L-2}^{k_2} CZ \frac{\partial \rho_{2L-2}}{\partial \theta}] \text{Tr}[CZ^\dagger \vec{\sigma}_{j,2L-2}^{k_2} CZ \frac{\partial \rho_{2L-2}}{\partial \theta}] \right) \quad (\text{S84})$$

$$= \sum_{k'_2} h_{k'_2} \mathbb{E}_\theta \left(\text{Tr}[\vec{\sigma}_{i,2L-2}^{k'_2} \frac{\partial \rho_{2L-2}}{\partial \theta}] \text{Tr}[\vec{\sigma}_{j,2L-2}^{k'_2} \frac{\partial \rho_{2L-2}}{\partial \theta}] \right) \quad (\text{S85})$$

$$\dots \quad (\text{S86})$$

$$= \sum_{k'_{2L}} h_{k'_{2L}} \text{Tr}[\vec{\sigma}_{i,0}^{k'_{2L}} \rho_0] \text{Tr}[\vec{\sigma}_{j,0}^{k'_{2L}} \rho_0] \quad (\text{S87})$$

Among these, the coefficients $h_{k_1}, h_{k_2}, h_{k'_2}, \dots, h_{k_{2L}}, h_{k'_{2L}}$ take the form $\pm \alpha^{g_1} \beta^{g_2} \gamma^{g_3}$, where $g_1, g_2, g_3 \in \mathbb{N}$. $\vec{\sigma}_{i,0}^{k'_{2L}}, \vec{\sigma}_{i,0}^{k_{2L}}, \dots, \vec{\sigma}_{i,2L-1}^{k_1}, \vec{\sigma}_{i,2L}, \vec{\sigma}_{j,0}^{k'_{2L}}, \vec{\sigma}_{j,0}^{k_{2L}}, \dots, \vec{\sigma}_{j,2L-1}^{k_1}, \vec{\sigma}_{j,2L}$ are all in the form of Pauli matrix tensor product. Furthermore, since \mathbf{O}_i and \mathbf{O}_j are both globally observable operators, and $\mathbf{O}_i \neq \mathbf{O}_j$, there exists $k \in [N]$ such that the Pauli matrix on the k -th qubit of $\sigma_{k,i,2L}$ and $\tilde{\sigma}_{k,j,2L}$ is one of the cases $\{X, Y; Y, X; X, Z; Z, X; Y, Z; Z, Y\}$. Next, we will prove that for all these combinations, $\mathbb{E}_{\theta} \left(\frac{\partial f_i(\theta)}{\partial \theta} \frac{\partial f_j(\theta)}{\partial \theta} \right) = 0$. Without loss of generality, let's assume that there exists k such that the k -th position of $\sigma_{k,i,2L}$ is X and the k -th position of $\tilde{\sigma}_{k,j,2L}$ is Z .

Next, let's consider the changes in observables. According to Lemma 1, 2, 3, and 4, after the last block's R_y rotation gate, regardless of the distribution followed by θ in $R_x(\theta)$, based on Eq. (S17), Eq. (S27) and Eq. (S37), the value at position k becomes $\{X, Z\}$ or $\{Z, X\}$, the coefficients for the other terms are zero. However, different distributions will result in varying coefficients in front of $\{X, Z\}$ or $\{Z, X\}$. $\{X, Z\}, \{Z, X\}$ remains $\{X, Z\}, \{Z, X\}$ or 0 after the R_x rotation gate, according to Eq. (S15), Eq. (S24) and Eq. (S34). If it's non-zero, according to Lemma 5, the CZ operation can transform the original X or Y into X or Y , without changing them into Z or I . Similarly, it cannot transform Z and I into X or Y . If, after the application of CZ , the original Pauli matrix undergoes a change, such as turning X into Y or Z into I , we refer to this process as a "flip." Clearly, for any observable $C = c_1 \otimes c_2 \otimes \dots \otimes c_n$, if it aims to achieve a "flip" operation at its k -th position, it must satisfy the condition that the Pauli matrix at the $(k-1)$ -th position belongs to X, Y , the Pauli matrix at the $(k+1)$ -th position belongs to I, Z , or the Pauli matrix at the $(k-1)$ -th position belongs to I, Z , and the Pauli matrix at the $(k+1)$ -th position belongs to Z, I . Therefore, after the CZ entanglement gate, its situation becomes one of $\{X, Z; Z, X; Y, Z; Z, Y; X, I; I, X; Y, I; I, Y\}$. Furthermore, taking partial derivatives with respect to any position $\theta_{q,n}$ only alters the coefficients in front, and it does not lead to the appearance of the four possible combinations $\{I, I; Z, Z; I, Z; Z, I\}$ for Pauli matrices.

This analysis applies to each block similarly. Consequently, it generates numerous terms, but in each term, on the k -th qubit, all possible situations that eventually arise are $\{X, Z; Z, X; Y, Z; Z, Y; X, I; I, X; Y, I; I, Y\}$. This implies that in $\vec{\sigma}_{i,0}^{k'_{2L}}, \vec{\sigma}_{j,0}^{k'_{2L}}$, there is at least one term with X or Y . Additionally, since $\langle 0|X|0\rangle = \langle 0|Y|0\rangle = \langle 1|X|1\rangle = \langle 1|Y|1\rangle = 0$, it follows that $\text{Tr}[\vec{\sigma}_{i,0}^{k'_{2L}} \rho_0] \text{Tr}[\vec{\sigma}_{j,0}^{k'_{2L}} \rho_0] = 0$. Therefore, we conclude that when $\sigma_{k,i,2L} = X$ and $\tilde{\sigma}_{k,j,2L} = Z$, Eq. (S87) equals 0.

In an analogous manner, when the initial Pauli matrix of the k -th qubit is $\{X, Y; Y, X; Y, Z; Z, X; Z, Y\}$, we can still obtain $\text{Tr}[\vec{\sigma}_{i,0}^{k'_{2L}} \rho_0] \text{Tr}[\vec{\sigma}_{j,0}^{k'_{2L}} \rho_0] = 0$. Only when the initial state is one of $\{X, X; Y, Y; Z, Z; Z, I; I, Z; I, I\}$, $\text{Tr}[\vec{\sigma}_{i,0}^{k'_{2L}} \rho_0] \text{Tr}[\vec{\sigma}_{j,0}^{k'_{2L}} \rho_0] \neq 0$. In light of the fact that both \mathbf{O}_i and \mathbf{O}_j are global observables, and $\mathbf{O}_i \neq \mathbf{O}_j$, it follows that there exists at least one position, such that the Pauli matrices at the k -th position of \mathbf{O}_i and \mathbf{O}_j belong to the set $\{X, Y; Y, X; Y, Z; Z, X; Z, Y\}$. Thus, for global observable operators \mathbf{O}_i and \mathbf{O}_j , $\mathbb{E}_{\theta} \left(\frac{\partial f_i(\theta)}{\partial \theta} \frac{\partial f_j(\theta)}{\partial \theta} \right) = 0$.

Following a similar analysis, we obtain $\mathbb{E}_{\theta} \left(\frac{\partial f_{i_1}(\theta)}{\partial \theta_{q,n}} \cdot \frac{\partial f_{i_2}(\theta)}{\partial \theta_{q,n}} \right) = \mathbb{E}_{\theta} \left(\frac{\partial f_{j_1}(\theta)}{\partial \theta_{q,n}} \cdot \frac{\partial f_{j_2}(\theta)}{\partial \theta_{q,n}} \right) = 0$. Thus, Eq. (S80) can be simplified to:

$$\mathbb{E}_{\theta} \|\nabla_{\theta} f(\theta)\|^2 = \sum_{q,n,i} E \left(\frac{\partial f_i(\theta)}{\partial \theta_{q,n}} \right)^2 + \sum_{q,n,j} E \left(\frac{\partial f_j(\theta)}{\partial \theta_{q,n}} \right)^2 \quad (\text{S88})$$

$$\geq \sum_{q,n} E \left(\frac{\partial f_1(\theta)}{\partial \theta_{q,n}} \right)^2 \quad (\text{S89})$$

$$\geq \frac{1}{4} - \frac{1}{8L} \quad (\text{S90})$$

Thus, we have completed the proof of the lemma.

Next, let's proceed with the proof of Theorem 2. Without loss of generality, we select \mathbf{O}_1 and initialize the parameters of the quantum circuit according to it. Next, we will expand $f(\theta)$ to obtain its expression:

$$\mathbb{E}_{\theta} \|\nabla_{\theta} f(\theta)\|^2 = \sum_{q,n} \mathbb{E}_{\theta} \left(\frac{\partial f(\theta)}{\partial \theta_{q,n}} \right)^2 \quad (\text{S91})$$

$$= \sum_{q,n} \mathbb{E}_{\theta} \left(\sum_{i_1} \frac{\partial f'_{i_1}(\theta)}{\partial \theta_{q,n}} - \sum_{j_1} \frac{\partial f'_{j_1}(\theta)}{\partial \theta_{q,n}} + \sum_{i_2} \frac{\partial f''_{i_2}(\theta)}{\partial \theta_{q,n}} - \sum_{j_2} \frac{\partial f''_{j_2}(\theta)}{\partial \theta_{q,n}} \right)^2 \quad (\text{S92})$$

$$= \sum_{q,n} \mathbb{E}_{\theta} \left(\sum_{i_1} \frac{\partial f'_{i_1}(\theta)}{\partial \theta_{q,n}} - \sum_{j_1} \frac{\partial f'_{j_1}(\theta)}{\partial \theta_{q,n}} \right)^2 + 2 \sum_{q,n} \mathbb{E}_{\theta} \left(\sum_{i_1} \frac{\partial f'_{i_1}(\theta)}{\partial \theta_{q,n}} - \sum_{j_1} \frac{\partial f'_{j_1}(\theta)}{\partial \theta_{q,n}} \right) \left(\sum_{i_2} \frac{\partial f''_{i_2}(\theta)}{\partial \theta_{q,n}} - \sum_{j_2} \frac{\partial f''_{j_2}(\theta)}{\partial \theta_{q,n}} \right) + \sum_{q,n} \mathbb{E}_{\theta} \left(\sum_{i_2} \frac{\partial f''_{i_2}(\theta)}{\partial \theta_{q,n}} - \sum_{j_2} \frac{\partial f''_{j_2}(\theta)}{\partial \theta_{q,n}} \right)^2, \quad (\text{S93})$$

where $f'_{i_1}(\theta) = \text{Tr}[\mathbf{O}'_{i_1} U(\theta) \rho_0 U(\theta)^\dagger]$, $f'_{j_1}(\theta) = \text{Tr}[\mathbf{O}'_{j_1} U(\theta) \rho_0 U(\theta)^\dagger]$, $f''_{i_2}(\theta) = \text{Tr}[\mathbf{O}''_{i_2} U(\theta) \rho_0 U(\theta)^\dagger]$, $f''_{j_2}(\theta) = \text{Tr}[\mathbf{O}''_{j_2} U(\theta) \rho_0 U(\theta)^\dagger]$. The notations \mathbf{O}'_{i_1} and \mathbf{O}'_{j_1} suggest that, in comparison to \mathbf{O}_1 , they simply involve replacing some Pauli matrices Z with I or vice versa. For instance, consider $X \otimes Y \otimes Z \otimes I$ and $X \otimes Y \otimes I \otimes Z$. On the other hand, \mathbf{O}''_{i_2} , \mathbf{O}''_{j_2} represent other observables.

Following similar analyses from Lemma 6, we determine that the second term in Eq. S93 is equal to 0. Now, let's expand the remaining terms. Therefore:

$$\mathbb{E}_{\theta} \|\nabla_{\theta} f(\theta)\|^2 = \sum_{q,n} \mathbb{E}_{\theta} \left(\left(\sum_{i_1} \frac{\partial f'_{i_1}(\theta)}{\partial \theta_{q,n}} - \sum_{j_1} \frac{\partial f'_{j_1}(\theta)}{\partial \theta_{q,n}} \right)^2 + \left(\sum_{i_2} \frac{\partial f''_{i_2}(\theta)}{\partial \theta_{q,n}} - \sum_{j_2} \frac{\partial f''_{j_2}(\theta)}{\partial \theta_{q,n}} \right)^2 \right) \quad (\text{S94})$$

$$\geq \sum_{q,n} \mathbb{E}_{\theta} \left(\sum_{i_1} \frac{\partial f'_{i_1}(\theta)}{\partial \theta_{q,n}} - \sum_{j_1} \frac{\partial f'_{j_1}(\theta)}{\partial \theta_{q,n}} \right)^2 \quad (\text{S95})$$

$$= \sum_{q,n,i_1} \mathbb{E}_{\theta} \left(\frac{\partial f'_{i_1}(\theta)}{\partial \theta_{q,n}} \right)^2 + \sum_{q,n,i'_1 \neq i_1} \mathbb{E}_{\theta} \left(\frac{\partial f'_{i'_1}(\theta)}{\partial \theta_{q,n}} \cdot \frac{\partial f'_{i_1}(\theta)}{\partial \theta_{q,n}} \right) - 2 \sum_{q,n,i_1,j_1} \mathbb{E}_{\theta} \left(\frac{\partial f'_{i_1}(\theta)}{\partial \theta_{q,n}} \cdot \frac{\partial f'_{j_1}(\theta)}{\partial \theta_{q,n}} \right) + \sum_{q,n,j_1} \mathbb{E}_{\theta} \left(\frac{\partial f'_{j_1}(\theta)}{\partial \theta_{q,n}} \right)^2 + \sum_{q,n,j'_1 \neq j_1} \mathbb{E}_{\theta} \left(\frac{\partial f'_{j'_1}(\theta)}{\partial \theta_{q,n}} \cdot \frac{\partial f'_{j_1}(\theta)}{\partial \theta_{q,n}} \right) \quad (\text{S96})$$

It is easy to see that all the cross terms in this expression differ in the positions where I and Z occur. Therefore, there exists a k such that the k -th position in $f'_{i_1}(\theta)$ and $f'_{j_1}(\theta)$ is either I, Z or Z, I . According to Eq. (S34) and Eq. (S36), we know that the third term in Eq. (S96) is equal to 0. Similarly, we can analyze the other cross terms in Eq. (S96) and conclude that they are all equal to 0. Therefore, we have:

$$\mathbb{E}_{\theta} \|\nabla_{\theta} f(\theta)\|^2 \geq \sum_{q,n,i_1} \mathbb{E}_{\theta} \left(\frac{\partial f'_{i_1}(\theta)}{\partial \theta_{q,n}} \right)^2 + \sum_{q,n,j_1} \mathbb{E}_{\theta} \left(\frac{\partial f'_{j_1}(\theta)}{\partial \theta_{q,n}} \right)^2 \quad (\text{S97})$$

Given that \mathbf{O}'_{i_1} and \mathbf{O}_1 differ only in certain terms that flip I to Z or Z to I , and during the initialization of quantum circuit parameters, the k -th position in \mathbf{O}_1 follows $\mathcal{G}_3(\sigma^2)$ if it is I or Z . Therefore, for all i_1 , $\sum_{q,n} \mathbb{E}_{\theta} \left(\frac{\partial f'_{i_1}(\theta)}{\partial \theta_{q,n}} \right)^2$ are all equal. According to Eq. (S42) and Eq. (S43), and employing a similar analysis to Theorem 1, we obtain:

$$\sum_{q,n} \mathbb{E}_{\theta} \left(\frac{\partial f'_{i_1}(\theta)}{\partial \theta_{q,n}} \right)^2 \geq \frac{1}{4} - \frac{1}{8L} \quad (\text{S98})$$

Thus, we have:

$$\mathbb{E}_{\theta} \|\nabla_{\theta} f(\theta)\|^2 \geq M \left(\frac{1}{4} - \frac{1}{8L} \right) \quad (\text{S99})$$

PROOF OF THEOREM 3

Without loss of generality, we select \mathbf{O}_1 and initialize according to \mathbf{O}_1 . Let $\mathbf{O}_1 = o_1^1 \otimes o_2^1 \otimes \dots \otimes o_N^1$. We expand $f(\theta)$ to obtain:

$$\mathbb{E}_{\theta} \|\nabla_{\theta} f(\theta)\|^2 = \sum_{q,n} \mathbb{E}_{\theta} \left(\frac{\partial f(\theta)}{\partial \theta_{q,n}} \right)^2 \quad (\text{S100})$$

$$= \sum_{q,n} \mathbb{E}_{\theta} \left(\sum_i \frac{\partial f'_i(\theta)}{\partial \theta_{q,n}} + \sum_j \frac{\partial f''_j(\theta)}{\partial \theta_{q,n}} \right)^2 \quad (\text{S101})$$

$$= \sum_{q,n} \mathbb{E}_{\theta} \left(\sum_i \frac{\partial f'_i(\theta)}{\partial \theta_{q,n}} \right)^2 + 2 \sum_{q,n} \mathbb{E}_{\theta} \left(\sum_{i,j} \frac{\partial f'_i(\theta)}{\partial \theta_{q,n}} \cdot \frac{\partial f''_j(\theta)}{\partial \theta_{q,n}} \right) + \sum_{q,n} \mathbb{E}_{\theta} \left(\sum_j \frac{\partial f''_j(\theta)}{\partial \theta_{q,n}} \right)^2 \quad (\text{S102})$$

$$\geq \sum_{q,n,i} \mathbb{E}_{\theta} \left(\frac{\partial f'_i(\theta)}{\partial \theta_{q,n}} \right)^2 + \sum_{q,n,i_1 \neq i_2} \mathbb{E}_{\theta} \left(\frac{\partial f'_{i_1}(\theta)}{\partial \theta_{q,n}} \cdot \frac{\partial f'_{i_2}(\theta)}{\partial \theta_{q,n}} \right) + 2 \sum_{q,n,i,j} \mathbb{E}_{\theta} \left(\frac{\partial f'_i(\theta)}{\partial \theta_{q,n}} \cdot \frac{\partial f''_j(\theta)}{\partial \theta_{q,n}} \right), \quad (\text{S103})$$

where $f'_i(\theta) = \text{Tr}[\mathbf{O}'_i U(\theta) \rho_0 U(\theta)^\dagger]$ and $f''_j(\theta) = \text{Tr}[\mathbf{O}'_j U(\theta) \rho_0 U(\theta)^\dagger]$. \mathbf{O}'_i implies that, compared to \mathbf{O}_1 , they might have operations that flip some I to Z or Z to I , while the rest of the Pauli matrices are the same. \mathbf{O}'_j represents observables that do not satisfy these conditions.

According to a similar analysis as in Lemma 6, we can see that the third term in Eq. (S103) is equal to 0. In the context of the final block, where the positions of I and Z in \mathbf{O}_1 follow Gaussian distributions $\mathcal{N}(0, \sigma^2)$, and considering that \mathbf{O}'_i , compared to \mathbf{O}_1 , only involves flipping Pauli I to Pauli Z or Pauli Z to Pauli I, we can apply a similar analysis as in Theorem 1. As a result, in the first term of Eq. (S103), for each \mathbf{O}'_i , we find that $\sum_{q,n} \mathbb{E}_{\theta} \left(\frac{\partial f'_i(\theta)}{\partial \theta_{q,n}} \right)^2 \geq \frac{1}{4} - \frac{1}{8L}$. For the second term in Eq. (S103), when $n \in P_{1:3}^{ij}$ and $q \in [2L-2]$, note that:

$$\begin{aligned} & \mathbb{E}_{\theta} \left(\frac{\partial f'_{i_1}(\theta)}{\partial \theta_{q,n}} \cdot \frac{\partial f'_{i_2}(\theta)}{\partial \theta_{q,n}} \right) \\ &= \mathbb{E}_{\theta} \left(\frac{\partial}{\partial \theta_{q,n}} \text{Tr}[\mathbf{O}'_{i_1} \rho_{2L}] \cdot \frac{\partial}{\partial \theta_{q,n}} \text{Tr}[\mathbf{O}'_{i_2} \rho_{2L}] \right) \end{aligned} \quad (\text{S104})$$

$$= \mathbb{E}_{\theta_1} \dots \mathbb{E}_{\theta_{2L}} \left(\frac{\partial}{\partial \theta_{q,n}} \text{Tr}[\mathbf{O}'_{i_1} R_{2L}(\theta_{2L}) \rho_{2L-1} R_{2L}^\dagger(\theta_{2L})] \cdot \frac{\partial}{\partial \theta_{q,n}} \text{Tr}[\mathbf{O}'_{i_2} R_{2L}(\theta_{2L}) \rho_{2L-1} R_{2L}^\dagger(\theta_{2L})] \right) \quad (\text{S105})$$

$$\geq \alpha^{S_1^{i_1 i_2} + S_3^{i_1 i_2}} \gamma^{S_{0,3}^{i_1 i_2}} \mathbb{E}_{\theta_1} \dots \mathbb{E}_{\theta_{2L-1}} \left(\frac{\partial}{\partial \theta_{q,n}} \text{Tr}[\mathbf{O}'_{3:i_1;1} \rho_{2L-1}] \cdot \frac{\partial}{\partial \theta_{q,n}} \text{Tr}[\mathbf{O}'_{3:i_2;1} \rho_{2L-1}] \right) \quad (\text{S106})$$

$$\begin{aligned} & \geq \alpha^{S_1^{i_1 i_2} + S_3^{i_1 i_2}} \gamma^{S_{0,3}^{i_1 i_2}} \mathbb{E}_{\theta_1} \dots \mathbb{E}_{\theta_{2L-1}} \left(\frac{\partial}{\partial \theta_{q,n}} \text{Tr}[\mathbf{O}'_{3:i_1;1} R_{2L-1}(\theta_{2L-1}) C Z_L \rho_{2L-2} C Z_L^\dagger R_{2L}^\dagger(\theta_{2L-1})] \right. \\ & \quad \left. \cdot \frac{\partial}{\partial \theta_{q,n}} \text{Tr}[\mathbf{O}'_{3:i_2;1} R_{2L-1}(\theta_{2L-1}) C Z_L \rho_{2L-2} C Z_L^\dagger R_{2L}^\dagger(\theta_{2L-1})] \right) \end{aligned} \quad (\text{S107})$$

$$\geq \alpha^{S_1^{i_1 i_2} + S_3^{i_1 i_2}} \alpha^{S_{1:3}^{i_1 i_2}} \gamma^{2S_{0,3}^{i_1 i_2}} \mathbb{E}_{\theta_1} \dots \mathbb{E}_{\theta_{2L-2}} \left(\frac{\partial}{\partial \theta_{q,n}} \text{Tr}[\mathbf{O}'_{3:i_1} C Z_L \rho_{2L-2} C Z_L^\dagger] \cdot \frac{\partial}{\partial \theta_{q,n}} \text{Tr}[\mathbf{O}'_{3:i_2} C Z_L \rho_{2L-2} C Z_L^\dagger] \right) \quad (\text{S108})$$

$$= \alpha^{S_1^{i_1 i_2} + S_3^{i_1 i_2}} \alpha^{S_{1:3}^{i_1 i_2}} \gamma^{2S_{0,3}^{i_1 i_2}} \mathbb{E}_{\theta_1} \dots \mathbb{E}_{\theta_{2L-2}} \left(\frac{\partial}{\partial \theta_{q,n}} \text{Tr}[\mathbf{O}'_{3:i_1} \rho_{2L-2}] \cdot \frac{\partial}{\partial \theta_{q,n}} \text{Tr}[\mathbf{O}'_{3:i_2} \rho_{2L-2}] \right) \quad (\text{S109})$$

$$\geq \alpha^{S_1^{i_1 i_2} + S_3^{i_1 i_2}} \alpha^{(2L-q-1)S_{1:3}^{i_1 i_2}} \gamma^{(2L-q)S_{0,3}^{i_1 i_2}} \mathbb{E}_{\theta_1} \dots \mathbb{E}_{\theta_q} \left(\frac{\partial}{\partial \theta_{q,n}} \text{Tr}[\mathbf{O}'_{3:i_1} \rho_q] \cdot \frac{\partial}{\partial \theta_{q,n}} \text{Tr}[\mathbf{O}'_{3:i_2} \rho_q] \right) \quad (\text{S110})$$

Similar to Eq. (S64), Eq. (S106) is derived from Eq. (S9), (S15), (S42) and (S44). Similarly, we obtain Eq. (S108). Eq. (S109) is simplified through Lemma 5. Continuing this analysis up to layer q , we arrive at Eq. (S110).

$$\begin{aligned} & \mathbb{E}_{\theta} \left(\frac{\partial f'_{i_1}(\theta)}{\partial \theta_{q,n}} \cdot \frac{\partial f'_{i_2}(\theta)}{\partial \theta_{q,n}} \right) \\ &= \mathbb{E}_{\theta} \left(\frac{\partial}{\partial \theta_{q,n}} \text{Tr}[\mathbf{O}'_{i_1} \rho_{2L}] \cdot \frac{\partial}{\partial \theta_{q,n}} \text{Tr}[\mathbf{O}'_{i_2} \rho_{2L}] \right) \end{aligned} \quad (\text{S111})$$

$$\geq \alpha^{S_1^{i_1 i_2} + S_3^{i_1 i_2}} \alpha^{(2L-q-1)S_{1:3}^{i_1 i_2}} \gamma^{(2L-q+1)S_{0,3}^{i_1 i_2}} \alpha^{S_{1:3}^{i_1 i_2} - 1} \beta \mathbb{E}_{\theta_1} \dots \mathbb{E}_{\theta_{q-1}} (\text{Tr}[\mathbf{O}'_{3:i_1} \rho_{q-1}] \text{Tr}[\mathbf{O}'_{3:i_2} \rho_{q-1}]) \quad (\text{S112})$$

$$\geq \alpha^{S_1^{i_1 i_2} + S_3^{i_1 i_2}} \alpha^{(2L-1)S_{1:3}^{i_1 i_2}} \gamma^{2LS_{0,3}^{i_1 i_2}} \beta \text{Tr}[\mathbf{O}'_{3:i_1} \rho_0] \text{Tr}[\mathbf{O}'_{3:i_2} \rho_0] \quad (\text{S113})$$

$$\geq \alpha^{2LS_{1:3}^{i_1 i_2} - 1} \gamma^{2LS_{0,3}^{i_1 i_2}} \beta \quad (\text{S114})$$

$$\geq (1-\sigma^2)^{2LS_{1:3}^{i_1 i_2} - 1} e^{-L\sigma^2 S_{0,3}^{i_1 i_2}} \sigma^2 (1-\sigma^2) \quad (\text{S115})$$

$$= \frac{1}{2LS} \left(1 - \frac{1}{2LS}\right)^{2LS_{1:3}^{i_1 i_2}} e^{-\frac{S_{0,3}^{i_1 i_2}}{2S}}, \quad (\text{S116})$$

Eq. (S111) to Eq. (S116) follow a similar analysis to Eq. (S69) and Eq. (S73). When $n \in P_{1:3}^{ij}$, a similar analysis reveals that when $q = 2L-1$,

$$\mathbb{E}_{\theta} \left(\frac{\partial f(\theta)}{\partial \theta_{q,n}} \right)^2 \geq \frac{1}{2LS} \left(1 - \frac{1}{2LS}\right)^{2LS_{1:3}^{ij}} e^{-\frac{S_{0,3}^{ij}}{2S}}, \quad (\text{S117})$$

and when $q = 2L$, $\mathbb{E}_{\theta} \left(\frac{\partial f(\theta)}{\partial \theta_{q,n}} \right)^2 \geq 0$. Fig. S3 and S4 illustrate the evolution of the first cross-terms in Eq. S103 for different configurations of Pauli matrices at each position. According to Lemma 5, CZ may execute a flip operation. Therefore, we discuss two scenarios: one where no flip occurs, as shown in Fig. S3, and another where CZ causes a flip of Pauli matrices, as depicted in Fig S4. As mentioned earlier, we find that if the k -th Pauli matrix is to undergo a flip operation, we require the $(k-1)$ -th position to have a Pauli matrix of X or Y , and the $(k+1)$ -th position to have a Pauli matrix of Z or I , or vice versa. Taking into account that some terms in the evolution of $iGO\rho$ may yield coefficients with negative signs, our specific setup ensures that when the coefficient for the preceding Pauli matrix becomes negative, the succeeding Pauli matrix will also inevitably have a negative coefficient. Consequently, the final coefficients are positive. When $n \notin P_{1:3}^{ij}$, i.e., $n \in P_0^{i,j}$, we can easily deduce that $\mathbb{E}_{\theta} \left(\frac{\partial f(\theta)}{\partial \theta_{q,n}} \right)^2 \geq 0$. In conclusion, we can draw the following conclusions:

$$\mathbb{E}_{\theta} \|\nabla_{\theta} f(\theta)\|_2^2 \geq M \left(\frac{1}{4} - \frac{1}{8L} \right) + \sum_{i \neq j=1}^M \frac{(2L-1)S_3^{ij}}{2LS} \left(1 - \frac{1}{2LS}\right)^{2LS_{1:3}^{ij}} e^{-\frac{S_{0,3}^{ij}}{2S}} + \sum_{q,n,j} E \left(\frac{\partial f_j''(\theta)}{\partial \theta_{q,n}} \right)^2 \quad (\text{S118})$$

$$\geq M \left(\frac{1}{4} - \frac{1}{8L} \right) + \sum_{i \neq j=1}^M \frac{(2L-1)S_3^{ij}}{2LS} \left(1 - \frac{1}{2LS}\right)^{2LS_{1:3}^{ij}} e^{-\frac{S_{0,3}^{ij}}{2S}} \quad (\text{S119})$$

ADDITIONAL NUMERICAL EXPERIMENTS AND DETAILS

Experiments with arbitrary global cost functions

Finally, we randomly generate some global observables to calculate their initial gradients. In this case, the cost function is given by $f(\theta) = \text{Tr}[(\sum_{i=1}^{10} \mathbf{O}_i - \sum_{j=1}^{10} \mathbf{O}_j)U(\theta)\rho_{in}U^\dagger(\theta)]$, where the Pauli matrices in \mathbf{O}_i and \mathbf{O}_j are randomly selected from $\{X, Y, Z\}$. We set L to be 2 and computed $\mathbb{E}_{\theta} \|\nabla_{\theta} f(\theta)\|_2^2$ for different numbers of qubits N . The results are presented in Table S4. Given that each term is global and excludes Pauli I , in this case, $M = 1$. Consequently, according to Theorem 2, our lower bound on $\mathbb{E}_{\theta} \|\nabla_{\theta} f(\theta)\|_2^2$ is 0.25. From the results, it is evident that with an increase in the number of qubits, the $\mathbb{E}_{\theta} \|\nabla_{\theta} f(\theta)\|_2^2$ for Gaussian, uniform, and reduced-domain distributions undergoes a sharp reduction. While our method also exhibits a decreasing trend in $\mathbb{E}_{\theta} \|\nabla_{\theta} f(\theta)\|_2^2$, it aligns closely with the outcome predicted by Theorem 2 and significantly surpasses other methods by several orders of magnitude.

TABLE S4. Comparison of initial gradients norm $\mathbb{E}_{\theta} \|\nabla_{\theta} f(\theta)\|_2^2$ for different methods at various numbers of qubits.

N	GMM	Gaussian	Uniform	Reduced-domain
5	1.26	0.99	2.02	1.21
10	0.75	2.86×10^{-2}	0.41	6.22×10^{-2}
15	0.73	1.92×10^{-7}	6.65×10^{-2}	8.56×10^{-4}
20	0.74	3.47×10^{-16}	8.78×10^{-3}	4.61×10^{-6}
25	0.74	2.55×10^{-23}	1.37×10^{-3}	6.87×10^{-8}

Simulated experiments in quantum chemistry

In the following, we explore the application of our initialization method to compute the ground-state energy of the LiH molecule, a benchmark in quantum chemistry. For an electronic system with N electrons distributed over M spin molecular orbitals, the initial state is the Hartree-Fock (HF) state:

$$|\Phi\rangle_{HF} = |\underbrace{11\dots 11}_{M} 00\dots 00\rangle.$$

In the LiH molecule, with an electron count of $N = 2$ and $M = 10$ free spin orbitals, simulating electronic structure problems on a quantum computer requires establishing a mapping that transforms fermionic operators of electrons into Pauli operators. Common mappings include the Jordan-Wigner (JW) transformation, Bravyi-Kitaev (BK) transformation, and Parity transformation. Here, we adopt the JW mapping to compute its ground-state energy.

We set the number of layers (L) to 10, 20, and 30, using a gradient descent optimizer with a learning rate of 0.01. Additionally, we consider the impact of the noise on the barren plateau problem by introducing a moderate amount of noise during training to simulate real-world quantum computer operation. We compare the evolution of the cost function and $\mathbb{E}_{\theta} \|\nabla_{\theta} f(\theta)\|_2^2$ during training when initializing parameters using GMM and uniform distribution $\mathcal{U}[-\pi, \pi]$. The results are shown in Fig. S5, S6, and S7. In each figure, (a) and (b) represent the condition without noise, while (c) and (d) represent the noisy condition. From the results, we observe that regardless of the value of L or the presence of noise, initializing parameters using the GMM method consistently provides a larger $\mathbb{E}_{\theta} \|\nabla_{\theta} f(\theta)\|_2^2$ at the beginning of training and it consistently stays much higher than the lower bound we have provided. This value remains relatively high before the convergence of the cost function, therefore, the GMM initialization ensures a rapid convergence. On the other hand, the uniform distribution $\mathcal{U}[-\pi, \pi]$ maintains a consistently lower level of gradient norm, resulting in a significantly slower convergence process.

Next, let's consider the impact of the parameter σ^2 in the GMM. In the main text, we set σ^2 to be $\frac{1}{2LS}$. We compare the training scenarios with different σ^2 values under noisy and noise-free conditions when $L = 10, 20, 30$. Here, σ^2 is chosen as $0.1 \times \frac{1}{2LS}$, $\frac{1}{2LS}$, and $10 \times \frac{1}{2LS}$. The results are shown in Fig. S8, S9, and S10.

As before, (a) and (b) represent noise-free conditions, while (c) and (d) represent scenarios with noise. The results in the figures indicate that when $\sigma^2 = 10 \times \frac{1}{2LS}$, the convergence of the cost function is significantly slower. On the other hand, when $\sigma^2 = 0.1 \times \frac{1}{2LS}$, although the cost function converges, its results are often inferior to the original case, especially in the presence of noise. We believe that as σ^2 increases, the peaks of the probability density function in the GMM become lower, and its distribution becomes closer to the uniform distribution, leading to a smaller KL divergence between them. Conversely, when σ^2 decreases, the peaks of the GMM's probability density function become higher. Therefore, the data becomes more concentrated around the peaks, making it less dispersed. This may be the reason why the convergence results are not as good as when $\sigma^2 = \frac{1}{2LS}$.

DISCUSSION REAMRK

According to Lemma 5, we observe that when Pauli matrices are limited to I and Z , the CZ gate does not alter their forms. In other words, $CZ^{\dagger}(o_i \otimes o_j)CZ = o_i \otimes o_j$ for all $o_i, o_j \in I, Z$. Therefore, CZ_l can be any combination of CZ gates, and it only changes the conditions for 'flip,' which does not affect our results. Also, although our method is specifically effective for the $R_x - R_y$ gate structure, it can be readily extended to other combinations of rotation gates. For instance, as shown in Theorem 2, if we interchange the positions of R_x and R_y in the arrangement of rotation gates, i.e., the arrangement is $R_y - R_x$, then we initialize the parameters of the last block according to Table S5, and the initialization of parameters in other layers follows the

distribution $\mathcal{G}_1(\sigma^2)$. Alternatively, when the rotation gates consist of three $R_x-R_y-R_x$ gates, under the same conditions as in Theorem 1, we initialize the parameters of the last block as shown in Table S6, and the initialization of parameters in other layers follows the distribution $\mathcal{G}_1(\sigma^2)$. In both cases, the results are consistent with those of Theorem 1. Certainly, our analysis method remains applicable when using CNOT to provide entanglement.

TABLE S5. For the R_y-R_x gate structure, we initialize the parameters θ in both $R_y(\theta)$ and $R_x(\theta)$ gates using a Gaussian distribution $\mathcal{G}_1(\sigma^2)$.

o_i	X	Y	Z	I
Init method of $R_x(\theta)$	$\mathcal{G}_2(\sigma^2)$	$\mathcal{G}_1(\sigma^2)$	$\mathcal{G}_3(\sigma^2)$	$\mathcal{G}_3(\sigma^2)$
Init method of $R_y(\theta)$	$\mathcal{G}_1(\sigma^2)$	$\mathcal{G}_2(\sigma^2)$	$\mathcal{G}_3(\sigma^2)$	$\mathcal{G}_3(\sigma^2)$

TABLE S6. For the $R_x-R_y-R_x$ gate structure, we initialize the parameters θ in both $R_y(\theta)$ and $R_x(\theta)$ gates using a Gaussian distribution $\mathcal{G}_1(\sigma^2)$.

o_i	X	Y	Z	I
Init method of first $R_x(\theta)$	$\mathcal{G}_3(\sigma^2)$	$\mathcal{G}_3(\sigma^2)$	$\mathcal{G}_3(\sigma^2)$	$\mathcal{G}_3(\sigma^2)$
Init method of $R_y(\theta)$	$\mathcal{G}_1(\sigma^2)$	$\mathcal{G}_2(\sigma^2)$	$\mathcal{G}_3(\sigma^2)$	$\mathcal{G}_3(\sigma^2)$
Init method of second $R_x(\theta)$	$\mathcal{G}_1(\sigma^2)$	$\mathcal{G}_2(\sigma^2)$	$\mathcal{G}_3(\sigma^2)$	$\mathcal{G}_3(\sigma^2)$

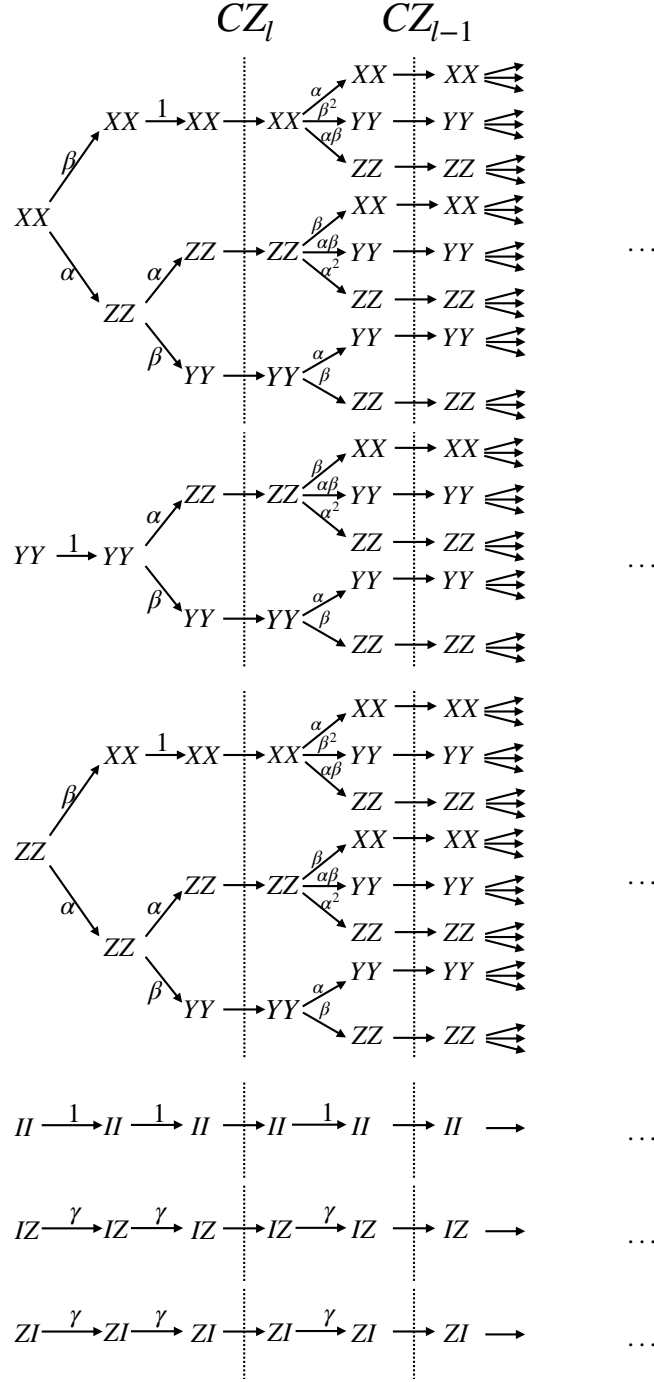


FIG. S3. At each position, depending on the different initial Pauli matrices, various terms are generated. This indicates that when the initial Pauli matrix at any position belongs to $\{XX, YY, ZZ, II, IZ, ZI\}$, it shows the transformation of the Pauli matrix and the corresponding coefficients. When the Pauli matrix undergoes a CZ gate, according to Lemma 5, it may involve flipping operations. Here, it illustrates the scenario when no flips exist, showcasing the changes in the Pauli matrix.

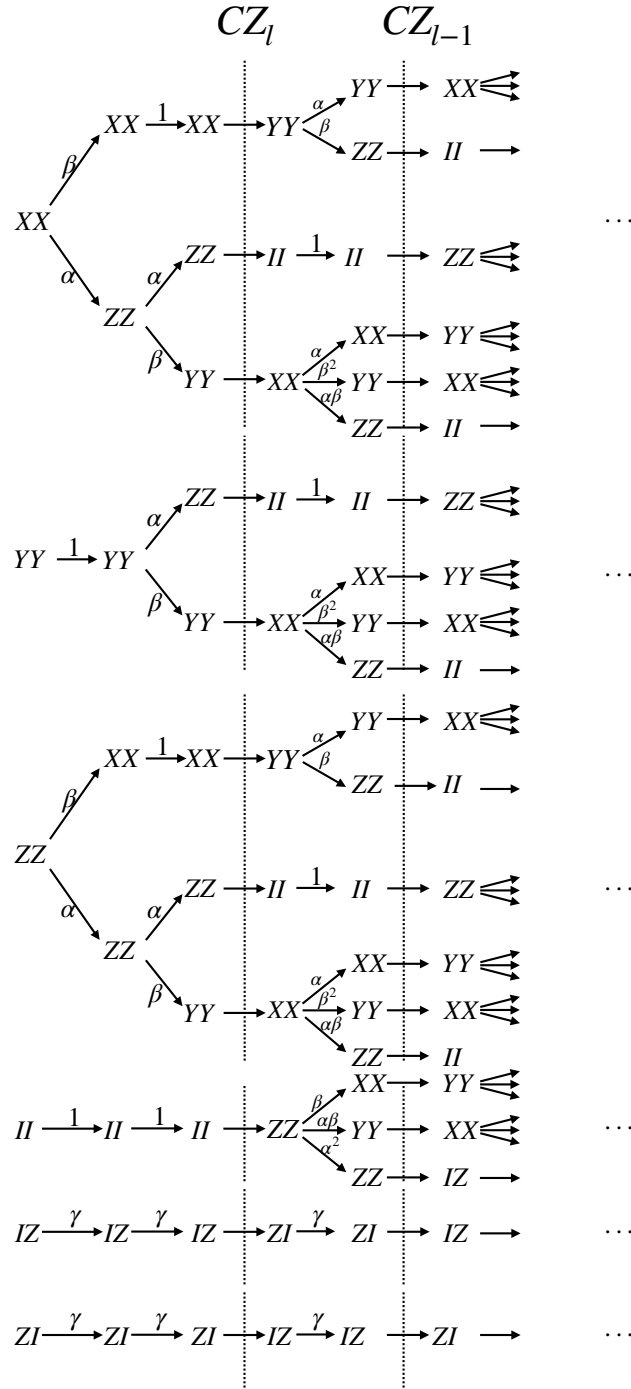


FIG. S4. As before, it illustrates changes in the Pauli matrix. However, in this case, we assume that the CZ gate introduces flip operations.

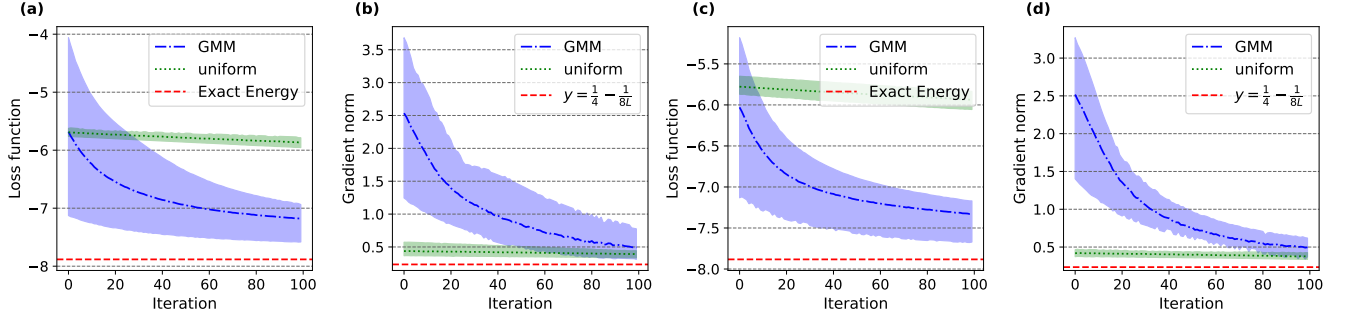


FIG. S5. When $L = 10$, we examine the variation of the cost function and $\mathbb{E}_{\theta} \|\nabla_{\theta} f(\theta)\|^2$ under noisy and noise-free conditions, using both uniform distribution ($\mathcal{U}[-\pi, \pi]$) and GMM-initialized parameters. Where (a) and (b) represent the noise-free scenario, while (c) and (d) represent the case with noise.

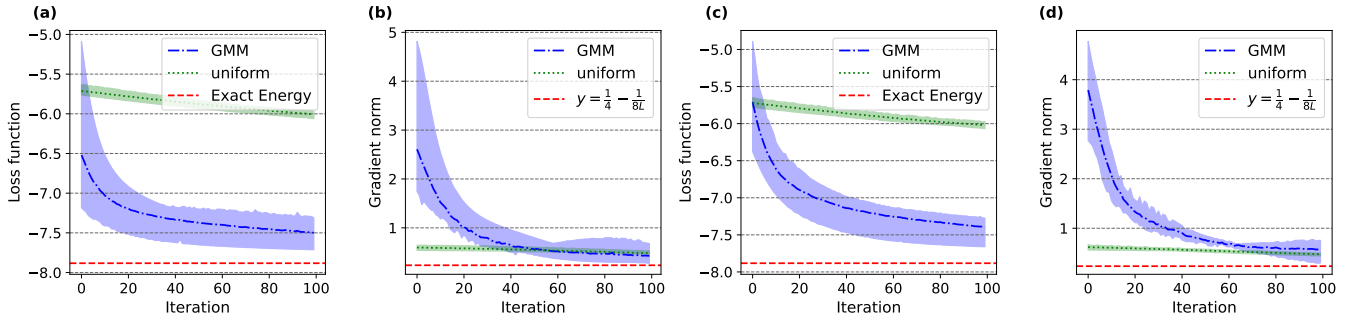


FIG. S6. When $L = 20$, (a) and (c) depict the loss function under noise-free and noisy conditions, respectively, with a uniform distribution ($\mathcal{U}[-\pi, \pi]$) and GMM-initialized parameters. On the other hand, (b) and (d) illustrate the changes in $\mathbb{E}_{\theta} \|\nabla_{\theta} f(\theta)\|^2$ under noise-free and noisy conditions, respectively.

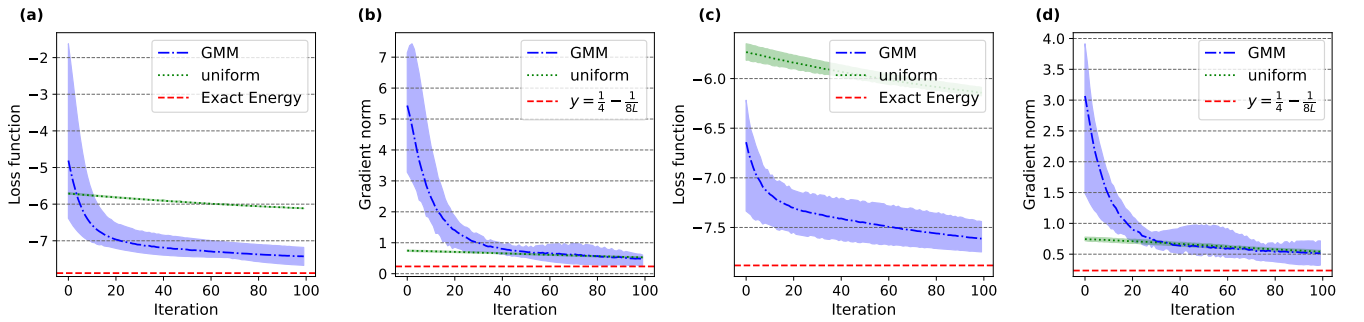


FIG. S7. When $L = 30$, (a) illustrates the variation of the loss under noise-free conditions; (b) depicts $\mathbb{E}_{\theta} \|\nabla_{\theta} f(\theta)\|^2$ under noise-free conditions; (c) shows the change in loss under noisy conditions; and (d) displays $\mathbb{E}_{\theta} \|\nabla_{\theta} f(\theta)\|^2$ under noisy conditions.

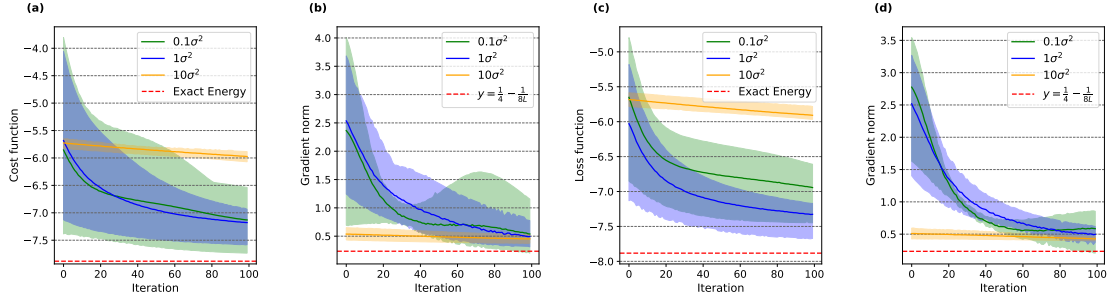


FIG. S8. In the configuration with $L = 10$, the impact of different σ^2 on training under noisy and noise-free conditions is depicted. Here, (a) and (b) represent the noise-free scenario, while (c) and (d) represent the noisy scenario.

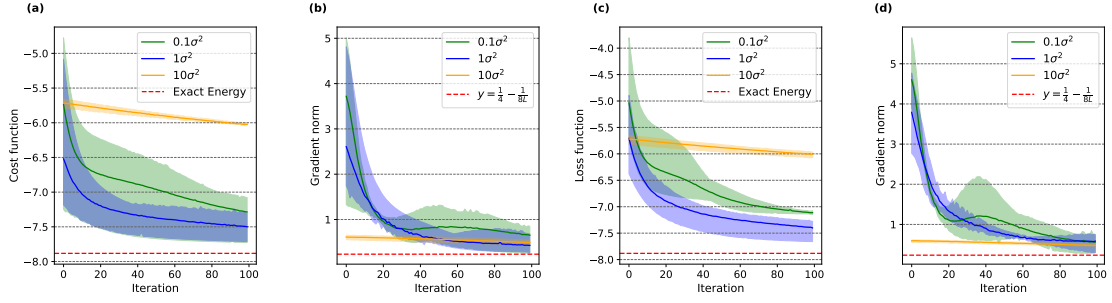


FIG. S9. For a 20-layer configuration, the impact of different σ^2 on training under noisy and noise-free conditions is depicted. Here, (a) and (b) represent the noise-free scenario, while (c) and (d) represent the noisy situation.

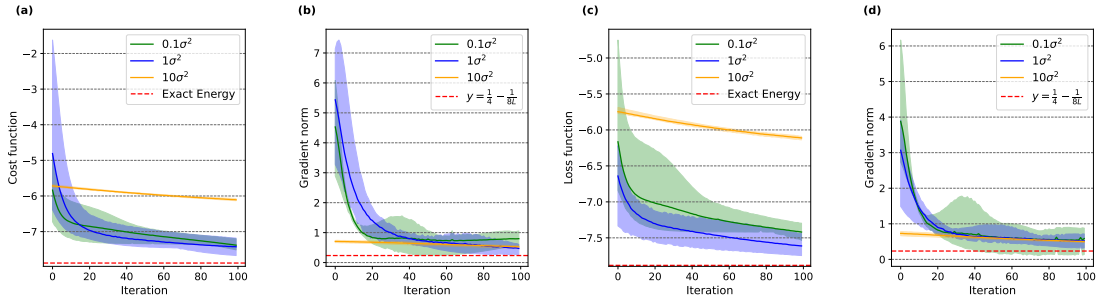


FIG. S10. In the $L = 30$ configuration, (a) and (b) illustrate the impact of different σ^2 on training under noise-free conditions, while (c) and (d) depict the influence of various σ^2 under noisy conditions.